enough to explain the positive results within the several minutes required to perform the picric acid test for cyanide.[30b]

The initial reaction between $Ag(OH)_4^-$ and thiocyanate most likely involves a nucleophilic attack of the reductant on the central Ag(III) ion. Like Pt(II), Pd(II), Cu(III), and Au(III), Ag(III) complexes have a low-spin d^8 electron configuration and are square planar. Nucleophilic attack on the Ag(III) site creates a five-coordinate intermediate complex as is characteristic of square-planar ligand substitution and seems important in other $Ag(OH)_4^-$ oxidations.[25] A large negative value of $\Delta S^{\ddagger}$ is common for this associative mechanism. In the intermediate, which is most likely to be S-bound,[40] the SCN^- transfers two electrons directly to the Ag(III), making the stable d^{10} electron configuration of Ag(I) and producing the SCN^+ moiety, which reacts rapidly with OH^-. There are, however, plausible alternatives to reactions 2 and 3, analogues of which have been considered for other $Ag(OH)_4^-$ systems. Direct bimolecular reaction between SCN^- and a bound hydroxyl could produce HOSCN with simultaneous reduction of the metal. A similar path has been proposed in the SCN^- reduction of halogold(III) complexes, resulting in neutral XSCN intermediates.[4] The linear structure of thiocyanate would, however, prohibit such intermediates if SCN and X (or OH) were both bound to the metal. We have discussed this possibility for the reactions of silver(III) and reduced oxoanions, and find that this path is not operative in those cases.[23]

Another alternative to HOSCN production involves the equilibrium replacement of a hydroxyl ion by SCN^- followed by attack of bulk OH^- on the $Ag(OH)_3(SCN)^-$ complex. This combination would be $[OH^-]$ independent as observed. Although this is certainly possible, the lack of evidence for complexation, which *has* been observed in other reactions,[24,26] offers no support for ligand substitution. Finally, questions concerning the actual production of SCN^+ in reaction 2 can be overcome if the nucleophilic attack of SCN^- on silver(III) were rate determining and followed by rapid reaction of OH^- with the five-coordinate intermediate.

Acknowledgment. We wish to thank the Donors of the Petroleum Research Fund, administered by the American Chemical Society, for support of this research.

(40) Golub, A. M.; Köhler, H.; Skopenko, V. V. *Chemistry of Pseudohalides*, Elsevier: Amsterdam, 1986; p 275.

Contribution from the Departments of Chemistry, University of Virginia, Charlottesville, Virginia 22901, University of North Carolina, Chapel Hill, North Carolina 27514, and University of Delaware, Newark, Delaware 19711

Synthesis and Structures of the $[MoFe_6S_6(CO)_{16}]^{2-}$, $[MoFe_4S_3(CO)_{13}(PEt_3)]^{2-}$, and $[Mo_2Fe_2S_2(CO)_{12}]^{2-}$ Ions: High-Nuclearity Mo–Fe–S Clusters as Potential Precursors to Models for the FeMo-Cofactor of Nitrogenase

P. A. Eldredge,[1a] K. S. Bose,[1b] D. E. Barber,[1b] R. F. Bryan,[1b] E. Sinn,[1b,c] A. Rheingold,[1d] and B. A. Averill*,[1b]

Received January 29, 1991

Reaction of $[Mo(CO)_4I_3]^-$ with 2–3 equiv of $[Fe_2S_2(CO)_6]^{2-}$ in THF produces two new Mo–Fe–S–CO clusters, the $[MoFe_6S_6(CO)_{16}]^{2-}$ (I) and $[MoFe_4S_3(CO)_{14}]^{2-}$ (II) ions, both of which have been structurally characterized, the latter as its mono(triethylphosphine) substitution product, $[MoFe_4S_3(CO)_{13}(PEt_3)]^{2-}$ (II-P). Crystallographic data: $(Ph_4As)_2$(I), triclinic, $P\bar{1}$ (No. 2), $Z = 2$, $a = 12.473$ (12) Å, $b = 12.836$ (13) Å, $c = 22.360$ (22) Å, $\alpha = 90.96$ (2)°, $\beta = 97.58$ (2)°, $\gamma = 99.52$ (2)°, $V = 3497$ Å^3, $R = 0.083$, $R_w = 0.094$, 9146 independent reflections with $I > 2.5\sigma(I)$; $(Et_4N)_2$(I), monoclinic, $P2_1/c$ (No. 14), $Z = 4$, $a = 19.275$ (7) Å, $b = 11.940$ (3) Å, $c = 20.975$ (1) Å, $\beta = 90.38$ (4)°, $V = 4827$ Å^3, $R = 0.038$, $R_w = 0.048$, 3872 independent reflections with $I > 3\sigma(I)$; $(Ph_4As)_2$(II-P), monoclinic, $P2_1/c$ (No. 14), $Z = 4$, $a = 18.124$ (4) Å, $b = 15.630$ (3) Å, $c = 24.665$ (5) Å, $\beta = 98.109$ (2)°, $V = 6917$ Å^3, $R = 0.063$, $R_w = 0.063$, 3874 independent reflections with $I > 5\sigma(I)$. Cluster I consists of a low-symmetry (C_1) arrangement of Fe atoms about a highly distorted trigonal-prismatic MoS_6 core, in which all sulfur atoms bridge to two or three Fe atoms. In one direction along a pseudo-2-fold axis of the trigonal prism are two Fe atoms at 2.74 and 2.77 Å from Mo, while the opposite tetragonal face is spanned by a zigzag chain of four Fe atoms, one of which at 2.68 Å is also bonded to Mo. The four-Fe chain contains one relatively long (2.74 Å) Fe–Fe interaction and a single bridging CO ligand, with terminal CO's completing the ligation to each Fe. The structure of I is essentially identical in both salts examined, suggesting that it arises from electronic considerations rather than crystal packing effects. The $MoFe_6S_6$ core stoichiometry of I together with the presence of three Fe atoms 2.7 Å from Mo makes it the closest synthetic approximation yet to the core stoichiometry and structure of the FeMo-cofactor of nitrogenase, suggesting that it may serve as a precursor to models for the FeMo-cofactor via oxidative decarbonylation reactions. Cluster II-P also exhibits a low-symmetry structure in which three new Mo–Fe interactions have been formed within an approximately square-pyramidal $MoS_3(CO)_2$ coordination sphere derived from coordination of two $[Fe_2S_2(CO)_6]^{2-}$ units to Mo with loss of one sulfur atom. The PEt_3 ligand is coordinated to the only Fe atom not bonded to Mo. The average Mo–S distance in both I and II-P is 2.43 Å, consistent with a Mo(II) formulation. Reaction of $[Mo(CO)_5I]^-$ with 1 equiv of $[Fe_2S_2(CO)_6]^{2-}$ results in the formation of cluster II in addition to a new cluster, the $[Mo_2Fe_2S_2(CO)_6]^{2-}$ ion (III), which has been characterized as its Ph_4As^+ salt. Crystallographic data for $(Ph_4As)_2$(III): monoclinic, $P2_1/m$ (No. 11), $Z = 4$, $a = 11.938$ (20) Å, $b = 16.729$ (30) Å, $c = 15.694$ (25) Å, $\beta = 111.45$ (50)°, $V = 2918$ Å^3, $R = 0.062$, $R_w = 0.058$, 3182 independent reflections with $I > 3\sigma(I)$. The structure of III consists of a centrosymmetric distorted octahedral $Mo_2Fe_2S_2$ core containing a planar Mo_2Fe_2 unit, with each Mo coordinated by three terminal CO's, each Fe coordinated by two terminal CO's, and a single CO bridging the Mo and Fe. The average Mo–S distance is 2.54 Å, consistent with a Mo(0) formulation. Plausible schemes for formation of clusters I–III are presented: cluster III arises from reaction of $[Fe_2S_2(CO)_6]^{2-}$ with *two* $[Mo(CO)_5I]^-$ ions; cluster II results from reaction of $[Mo(CO)_4I_3]^-$ with the dimeric disulfide-containing species $[Fe_4S_4(CO)_{12}]^{2-}$ produced in situ by oxidation of $[Fe_2S_2(CO)_6]^{2-}$; and cluster III requires the reaction of $[Mo(CO)_4I_3]^-$ with *both* $[Fe_2S_2(CO)_6]^{2-}$ and $[Fe_4S_4(CO)_{12}]^{2-}$. The implications of clusters I–III for the structure of the FeMo-cofactor of nitrogenase and as potential precursors to detailed models for the FeMo-cofactor are discussed.

The iron–molybdenum cofactor (FeMo-co) of nitrogenase[2] is arguably the most complex metal cluster to occur in biological systems. It contains one molybdenum atom, six to seven iron atoms, eight to ten sulfur atoms,[2,3] and one molecule of homo-

0020-1669/91/1330-2365$02.50/0

citrate,[4] which together form a small, anionic dissociable unit that is crucial to enzymatic reduction of dinitrogen to ammonia, probably by providing the actual site for N_2 binding and reduction.[5] The complexity of FeMo-co is suggested by genetic studies of nitrogen-fixing bacteria, which have implicated at least six genes and their protein products as necessary for FeMo-co biosynthesis.[6] Despite the application of a wide array of physical methods,[7] including Mössbauer,[8,9] ENDOR and EPR,[10] EXAFS,[11,12] XANES,[11a] CD and MCD,[13] and ^{19}F NMR[14] spectroscopy and magnetic susceptibility[15] and electrochemical[16] measurements, the structure of FeMo-co remains an enigma and constitutes one of the major unresolved problems in contemporary bioinorganic chemistry.

Complementary in nature to spectroscopic studies of metallobiomolecules, the synthetic analogue approach has provided significant insights into the nature of biologically active metal sites.[17] Its application to the problem of FeMo-co structure (an example of "speculative modeling" in the nomenclature of Hill[18]) has resulted in the preparation and characterization of a wide variety of novel Mo–Fe–S clusters over the past 10 years,[19] but until very recently none of the synthetic clusters have closely approached the correct Mo–Fe–S stoichiometry. Synthetic efforts to date have utilized two closely related approaches, neither of which is obviously biomimetic: "spontaneous self-assembly" of clusters from mononuclear starting materials and "fragment condensation reactions", utilizing more complex polynuclear species as starting materials. Early attempts at synthetic models for FeMo-co utilized the former approach, based on the reaction of MoS_4^{2-} with a variety of mononuclear iron sources, and produced either the well-characterized $MoFe_3S_4$ "cubane"[19a,b] or "linear"[19a-c,e] MoS_2Fe units with maximum Fe/Mo ratios of 3.5 and 2, respectively, depending upon the presence or absence of excess thiolate in the reaction medium. (Although MoS_4^{2-} has been shown to be produced in vivo under anaerobic conditions by rumen bacteria, its presence or intermediacy in nitrogen-fixing bacteria has not been demonstrated.) The lack of success in obtaining higher nuclearity clusters via this approach, the thermodynamic sink provided by complexes containing discrete tetrathiomolybdate units (e.g., $[Fe(S_2MoS_2)_2]^{3-}$),[20] and the lack of alternative mononuclear molybdenum starting materials containing nucleophilic sulfides has recently led to examination of alternative strategies in which the Mo–S–Fe unit is formed by attack of a nucleophilic iron–sulfide unit upon a variety of molybdenum starting materials containing easily displaced ligands. Because all of the iron–sulfide species utilized to date are at least binuclear, this has led naturally

(1) (a) University of North Carolina. Current address: Department of Chemistry, University of Virginia, Charlottesville, VA 22901. (b) University of Virginia. (c) Current address: School of Chemistry, University of Hull, Cottingham Road, Hull HU6 7RX, U.K. (d) University of Delaware.

(2) Shah, V. K.; Brill, W. J. *Proc. Natl. Acad. Sci. U.S.A.* **1977**, *74*, 3249.

(3) (a) Burgess, B. K.; Jacobs, D. R.; Stiefel, E. I. *Biochim. Biophys. Acta* **1980**, *614*, 196. (b) Yang, S. S.; Pan, W.-H.; Friesen, G. D.; Burgess, B. K.; Corbin, J. L.; Stiefel, E. I.; Newton, W. E. *J. Biol. Chem.* **1982**, *257*, 8042. (c) Nelson, M. J.; Levy, M. A.; Orme-Johnson, W. H. *Proc. Natl. Acad. Sci. U.S.A.* **1983**, *80*, 147. (d) Stiefel, E. I.; Cramer, S. P. In *Molybdenum Enzymes*; Spiro, T., Ed.; Wiley-Interscience: New York, 1985; p 89. (e) Frank, P.; Gheller, S. F.; Newton, W. E.; Hodgson, K. O. *Biochem. Biophys. Res. Commun.* **1989**, *163*, 746. (f) McLean, P. A.; Wink, D. A.; Chapman, S. K.; Hickman, A. B.; McKillop, D. M.; Orme-Johnson, W. H. *Biochemistry* **1989**, *28*, 9402. (g) Wink, D. A.; McLean, P. A.; Hickman, A. B.; Orme-Johnson, W. H. *Biochemistry* **1989**, *28*, 9407.

(4) Hoover, T. R.; Imperial, J.; Ludden, P. W.; Shah, V. K. *Biochemistry* **1989**, *28*, 2768.

(5) (a) Burgess, B. K. In *Advances in Nitrogen Fixation Research*; Veeger, C., Newton, W. E., Eds.; Nijhoff-Junk-Pudoc: Dordrecht, The Netherlands, 1983; p 103. (b) Nelson, M. J.; Lindahl, P. A.; Orme-Johnson, W. H. *Adv. Inorg. Biochem.* **1982**, *4*, 1. (c) Burgess, B. K.; Newton, W. E. In *Nitrogen Fixation, The Chemical-Biochemical-Genetic Interface*; Müller, A., Newton, W. E., Eds.; Plenum Press: New York, 1983; p 83. (d) Burgess, B. K. In *Nitrogen Fixation Research Progress*; Evans, H. J., Bottomley, P. J., Newton, W. E., Eds.; Martinus Nijhoff Publishers: Dordrecht, The Netherlands, 1985; p 543. (e) Burgess, B. K. In *Molybdenum Enzymes*; Spiro, T., Ed.; Wiley-Interscience: New York, 1985; p 161. (f) Burgess, B. K. *Chem. Rev.* **1990**, *90*, 1377.

(6) Hoover, T. R.; Imperial, J.; Ludden, P. W.; Shah, V. K. *Biofactors* **1988**, *1*, 199.

(7) (a) Stephens, P. J. In *Molybdenum Enzymes*; Spiro, T., Ed.; Wiley-Interscience: New York, 1985; p 117. (b) Orme-Johnson, W. H. *Annu. Rev. Biophys. Biophys. Chem.* **1985**, *14*, 419.

(8) (a) Zimmerman, R.; Münck, E.; Brill, W. J.; Shah, V. K.; Henzl, M. T.; Rawlings, J.; Orme-Johnson, W. H. *Biochim. Biophys. Acta* **1978**, *537*, 185. (b) Huynh, B. H.; Münck, E.; Orme-Johnson, W. H. *Biochim. Biophys. Acta* **1979**, *576*, 192. (c) Huynh, B. H.; Henzl, M. T.; Christner, J. A.; Zimmerman, R.; Orme-Johnson, W. H.; Münck, E. *Biochim. Biophys. Acta* **1980**, *623*, 124. (d) McLean, P. A.; Papaefthymiou, V.; Orme-Johnson, W. H.; Münck, E. *J. Biol. Chem.* **1987**, *262*, 12900. (e) Lindahl, P. A.; Papaefthymiou, V.; Orme-Johnson, W. H.; Münck, E. *J. Biol. Chem.* **1988**, *263*, 19412.

(9) (a) Smith, B. E.; O'Donnell, M. J.; Lang, G.; Spartalian, K. *Biochem. J.* **1980**, *191*, 449. (b) Dunham, W. R.; Hagen, W. R.; Braaksma, A.; Grande, H. J.; Haaker, H. *Eur. J. Biochem.* **1985**, *146*, 497. (c) Newton, W. E.; Gheller, S. F.; Sands, R. H.; Dunham, W. R. *Biochem. Biophys. Res. Commun.* **1989**, *162*, 882.

(10) (a) Hoffman, B. M.; Venters, R. A.; Roberts, J. E.; Nelson, M.; Orme-Johnson, W. H. *J. Am. Chem. Soc.* **1982**, *104*, 4711. (b) Hoffman, B. M.; Roberts, J. E.; Orme-Johnson, W. H. *J. Am. Chem. Soc.* **1982**, *104*, 860. (c) Thomann, H.; Morgan, T. V.; Jin, H.; Burgmayer, S. J. N.; Bare, R. E.; Stiefel, E. I. *J. Am. Chem. Soc.* **1987**, *109*, 7913. (d) True, A. E.; Nelson, M. J.; Venters, R. A.; Orme-Johnson, W. H.; Hoffman, B. M. *J. Am. Chem. Soc.* **1988**, *110*, 1935. (e) Euler, W. B.; Martinsen, J.; McDonald, J. W.; Watt, G. D.; Wang, Z.-C. *Biochemistry* **1984**, *23*, 3021. (f) George, G. N.; Bare, R. E.; Jin, H.; Stiefel, E. I.; Prince, R. C. *Biochem. J.* **1989**, *262*, 349.

(11) (a) Cramer, S. P.; Hodgson, K. O.; Gillum, W. O.; Mortenson, L. E. *J. Am. Chem. Soc.* **1978**, *100*, 3398. (b) Cramer, S. P.; Gillum, W. O.; Hodgson, K. O.; Mortenson, L. E.; Stiefel, E. I.; Chisnell, J. R.; Brill, W. J.; Shah, V. K. *J. Am. Chem. Soc.* **1978**, *100*, 3814. (c) Flank, A. M.; Weininger, M.; Mortenson, L. E.; Cramer, S. P. *J. Am. Chem. Soc.* **1986**, *108*, 1049. (d) Conradson, S. D.; Burgess, B. K.; Newton, W. E.; Mortenson, L. E.; Hodgson, K. O. *J. Am. Chem. Soc.* **1987**, *109*, 7507. (e) Hedman, B.; Frank, P.; Gheller, S. F.; Roe, A. L.; Newton, W. E.; Hodgson, K. O. *J. Am. Chem. Soc.* **1988**, *110*, 3798. (f) Conradson, S. D.; Burgess, B. K.; Vaughn, S. A.; Roe, A. L.; Hedman, B.; Hodgson, K. O.; Holm, R. H. *J. Biol. Chem.* **1989**, *264*, 15967. (g) Conradson, S. D.; Burgess, B. K.; Newton, W. E.; Hodgson, K. O.; McDonald, J. W.; Rubinson, J. F.; Gheller, S. F.; Mortenson, L. E.; Adams, M. W. W.; Mascharak, P. D.; Armstrong, W. A.; Holm, R. H. *J. Am. Chem. Soc.* **1985**, *107*, 7935.

(12) (a) Antonio, M. R.; Averill, B. A.; Groh, S. E.; Kauzlarich, S. M.; Lindahl, P. A.; Nelson, M. J.; Orme-Johnson, W. H.; Teo, B.-K. *J. Am. Chem. Soc.* **1982**, *104*, 4703. (b) Arber, J. M.; Flood, A. C.; Garner, C. D.; Gormal, C. A.; Hasnain, S. S.; Smith, B. E. *Biochem. J.* **1988**, *252*, 421.

(13) (a) Stephens, P. J.; McKenna, C. E.; Smith, B. E.; Nguyen, H. T.; McKenna, M. C.; Thomson, A. J.; Devlin, F.; Jones, J. B. *Proc. Natl. Acad. Sci. U.S.A.* **1979**, *76*, 2585. (b) Stephens, P. J.; McKenna, C. E.; McKenna, M. C.; Nguyen, H. T.; Devlin, F. *Biochemistry* **1981**, *20*, 2857. (c) Johnson, M. K.; Thomson, A. J.; Robinson, A. E.; Smith, B. E. *Biochim. Biophys. Acta* **1981**, *671*, 61.

(14) (a) Mascharak, P. K.; Smith, M. C.; Armstrong, W. H.; Burgess, B. K.; Holm, R. H. *Proc. Natl. Acad. Sci. U.S.A.* **1982**, *79*, 7056. (b) Conradson, S. D.; Burgess, B. K.; Holm, R. H. *J. Biol. Chem.* **1988**, *263*, 13743.

(15) (a) Smith, J. P.; Emptage, M. H.; Orme-Johnson, W. H. *J. Biol. Chem.* **1982**, *257*, 2310. (b) Day, E. P.; Kent, T. A.; Lindahl, P. A.; Münck, E.; Orme-Johnson, W. H.; Roder, H.; Roy, A. *Biophys. J.* **1987**, *52*, 837.

(16) (a) Watt, G. D.; Burns, A.; Lough, S.; Tennent, D. L. *Biochemistry* **1980**, *19*, 4926. (b) Morgan, T. V.; Mortenson, L. E.; McDonald, J. W.; Watt, G. D. *J. Inorg. Biochem.* **1988**, *33*, 111. (c) Schultz, F. A.; Gheller, S. F.; Burgess, B. K.; Lough, S.; Newton, W. E. *J. Am. Chem. Soc.* **1985**, *107*, 5364. (d) Schultz, F. A.; Gheller, S. F.; Newton, W. E. *Biochem. Biophys. Res. Commun.* **1988**, *152*, 629. (e) Newton, W. E.; Gheller, S. F.; Feldman, B. J.; Dunham, W. R.; Schultz, F. A. *J. Biol. Chem.* **1989**, *264*, 1924. (f) Shultz, F. A.; Feldman, B. J.; Gheller, S. F.; Newton, W. E. *Inorg. Chim. Acta* **1990**, *170*, 115.

(17) Ibers, J. A.; Holm, R. H. *Science (Washington, D.C.)* **1980**, *209*, 223.

(18) Hill, H. A. O. *Chem. Br.* **1976**, *12*, 119.

(19) (a) Holm, R. H.; Simhon, E. D. In *Molybdenum Enzymes*; Spiro, T., Ed.; Wiley-Interscience: New York, 1985; p 1. (b) Averill, B. A. *Struct. Bonding (Berlin)* **1983**, *53*, 59. (c) Coucouvanis, D. In *Nitrogen Fixation, The Chemical-Biochemical-Genetic Interface*; Müller, A., Newton, W. E., Eds.; Plenum Press: New York, 1983; p 211. (d) Garner, C. D.; Acott, S. R.; Christou, G.; Collison, D.; Mabbs, F. E.; Petrouleas, V.; Pickett, C. J. In *Nitrogen Fixation, The Chemical-Biochemical-Genetic Interface*; Müller, A., Newton, W. E., Eds.; Plenum Press: New York, 1983; p 245. (e) Coucouvanis, D. *Acc. Chem. Res.* **1981**, *14*, 201.

(20) (a) Coucouvanis, D.; Simhon, E. D.; Baenziger, N. C. *J. Am. Chem. Soc.* **1980**, *102*, 6646. (b) Friesen, G. D.; McDonald, J. W.; Newton, W. E.; Euler, W. B.; Hoffman, B. M. *Inorg. Chem.* **1983**, *22*, 2202.

to the exploration of fragment condensation reactions.

Two distinct variants of this strategy have been examined, both of which use abiological CO ligands on Mo and/or Fe. One has utilized the reaction of $Mo(CO)_3(MeCN)_3$ either to cap the hexagonal prismatic $[Fe_6S_6L_6]^{n-}$ clusters at both ends (or to induce rearrangement of $[Fe_4S_4L_4]^{2-}$ clusters), giving the "doubly capped" hexamers with $[Mo(CO)_3]_2Fe_6S_6$ cores,[21] or to induce rearrangement of the linear $[Fe_3S_4(SR)_4]^{3-}$ cluster to produce a cubane cluster with an $Mo(CO)_3Fe_3S_4$ core.[22] In contrast, our laboratory has examined the reaction of the $[Fe_2S_2(CO)_6]^{2-}$ ion,[23] a binuclear species known to possess highly reactive nucleophilic bridging sulfides capable of coordinating to a metal,[24] with a variety of molybdenum–halide reagents. In addition to producing a wide variety of new Fe–S carbonyl clusters,[25] this chemistry has resulted in the first examples of high-nuclearity synthetic Mo–Fe–S clusters with Fe/Mo ratios ≥5. Examples reported to date include the following: the $[MoOFe_5S_6(CO)_{12}]^{2-}$ ion,[26] possessing both a novel triply bridged MoS_2Fe_2 unit and a $(\mu_3\text{-}S)_2Fe_3S_2Mo$ unit containing a discrete 3Fe core; the $[MoFe_6S_6(CO)_{16}]^{2-}$ ion,[27] containing a highly distorted $MoFe_6S_6$ core with three Mo–Fe bonding interactions; and the $[MoFe_5S_6(CO)_6L_3]^{n-}$ clusters containing an $MoFe_3S_4$ cubane capped by an $Fe_2S_2(CO)_6$ unit.[28]

Despite the ubiquitous presence of distinctly abiological CO ligands, the Mo–Fe–S clusters produced to date by fragment condensation reactions are significant for three reasons. First, and most obviously, among them are the first synthetic clusters to approximate the core (Mo,Fe,S) stoichiometry observed for FeMo-co. Thus, these clusters may well serve as high-nuclearity Mo–Fe–S precursors to more detailed models for FeMo-co via decarbonylation reactions; some success along these lines has been reported.[28] Second, the clusters produced exhibit in some cases novel structural features that may offer insights into FeMo-co structure. Third, the area of high-nuclearity metal–carbonyl clusters has been the object of intense investigation in recent years, and the extension of chemistry developed for metals such as Os, Rh, and Ir to metals such as Mo and Fe is an interesting problem in synthetic cluster chemistry per se.

Herein we report full details of the synthesis and structure of compounds containing the $[MoFe_6S_6(CO)_{16}]^{2-}$ anion, as well as data indicating that the low-symmetry structure is dictated by electronic factors, plus the synthesis and structure of two new Mo–Fe–S clusters. In addition, we present plausible mechanistic conjectures for the assembly of all the title clusters. A portion of this work has appeared in preliminary form.[27]

Experimental Section

Methods and Materials. All operations were carried out under an atmosphere of pure, dry dinitrogen that had been purified by passage over hot BASF catalyst R3-11 and supported P_2O_5 (Aquasorb). Solvents and reagents were degassed by repeated evacuation and flushing with dry dinitrogen. Acetonitrile, tetrahydrofuran (THF), and 2-propanol were distilled from CaH_2, $LiAlH_4$ or sodium benzophenone ketyl, and Al(O-*i*-Pr)$_3$, respectively. Hexane was purified by washing with 5% v/v H_2SO_4, followed by water, and then drying over $MgSO_4$ and distilling from CaH_2. The following compounds were prepared by published procedures or modifications thereof as described below: $Fe_2S_2(CO)_6$,[29] $(Ph_4As)_2[Fe_4S_4(CO)_{12}]$,[30] $(Et_4N)[Mo(CO)_5I]$,[31] $(Et_4N)[Mo(CO)_4I_3]$.[32] All other compounds were reagent grade and were used as received. Microanalyses were performed by Galbraith Laboratories, Inc., Knoxville, TN.

$Fe_2S_2(CO)_6$. To 120 mL of a degassed solution of 50% aqueous KOH in 300 mL of CH_3OH was added 30 mL (228 mmol) of $Fe(CO)_5$. The solution was mechanically stirred and, after 15 min, cooled to 0 °C. Stirring was continued while 69 g (2.16 mol) of sulfur was added. After an additional 15 min, 750 mL of water and 1500 mL of pentane were added. This mixture was cautiously acidified with 600 mL of 25% HCl, evolving H_2S, while the reaction vessel was vented into approximately 500 mL of 50% aqueous KOH. The mixture was filtered in air and the solid rinsed with additional pentane; then the pentane extracts were washed with water and separated from the aqueous layer. Evaporation of the pentane layer gave a red oil that crystallized in vacuo. The solid product was sublimed at 40 °C under a vacuum of 0.01 Torr to give a crystalline product in 27% yield (10.2 g).

$(Et_4N)[Mo(CO)_5I]$. To 400 mL of degassed diglyme were added 12 g (45 mmol) of $Mo(CO)_6$ and 9.5 g (37 mmol) of 98% tetraethylammonium iodide. This slurry was stirred, a condenser attached, and the slurry heated to 120 °C in an oil bath. The nitrogen flow was stopped as decarbonylation commenced. After a reaction time of 90 min, the resulting deep yellow solution was filtered while hot. The yellow product was precipitated by the addition of 250 mL of hexane to the cooled filtrate and was collected by filtration; unreacted $Mo(CO)_6$ was sublimed from the product in vacuo. Yield: 86% (15.3 g).

$(Et_4N)[Mo(CO)_4I_3]$. Solid iodine (3.6 g; 14 mmol) was slowly added to a solution of 7.0 g (14 mmol) of $(Et_4N)[Mo(CO)_5I]$ in 150 mL of glyme under a nitrogen purge. The solution turned from deep yellow to golden brown as the reaction progressed and CO was evolved. The product was precipitated upon completion of the reaction by the addition of 400 mL of hexane. The slurry was cooled to 0 °C, and the solid product isolated by filtration. Yield: 93% (9.3 g).

Physical Measurements. All samples were handled under anaerobic conditions. Infrared spectra were obtained on either a Nicolet 10 DX or a Mattson Cygnus spectrophotometer, while optical spectra were measured on either a Cary 219 or a Cary 17 spectrophotometer. ^1H NMR spectra were obtained on a Nicolet QE-300 spectrometer, and magnetic susceptibility measurements were performed on an SHE SQUID susceptometer.

Cluster Syntheses. A. $(Ph_4As)_2[MoFe_6S_6(CO)_{16}]$, $(Ph_4As)_2$(I). A red solution of 1.5 g (4.4 mmol) of $Fe_2S_2(CO)_6$ in 100 mL of THF was cooled to −78 °C in an *i*-PrOH/dry ice bath. To this solution was added 9.0 mL of 1.0 M $LiEt_3BH$, corresponding to 2.0 equiv, in 0.5-mL increments. After completion of the reduction to $[Fe_2S_2(CO)_6]^{2-}$, a solution of 1.4 g (2.2 mmol) of $(Et_4N)[Mo(CO)_4I_3]$ in 50 mL of THF was added dropwise. The initial dark green solution changed to dark brown as the reaction progressed. This reaction mixture was allowed to warm to room temperature and filtered, and the solvent was removed in vacuo. The resulting oil was dissolved in approximately 100 mL of MeOH; then 2.5 g (6.0 mmol) of Ph_4AsCl in 100 mL of MeOH was added dropwise. The resulting precipitate was filtered out, washed with three aliquots of MeOH, and then dissolved in a minimum volume of CH_3CN. 2-Propanol was added dropwise to this solution. At the point of incipient crystallization, the solution was heated to 40 °C, stoppered, and slowly cooled to −20 °C. The product precipitated as dark brown crystals. These were collected by filtration and washed with three aliquots of *i*-PrOH. Yield: 30% (1.2 g). Anal. Calcd for $C_{64}H_{40}As_2Fe_6MoO_{16}S_6$: C, 41.82; H, 2.19; As, 8.15; Fe, 18.23; Mo, 5.22; S, 10.47. Found: C, 41.74; H, 2.27; As, 8.10; Fe, 17.56; Mo, 5.23; S, 10.72. IR (MeCN), cm^{-1} (ν(CO)): 2048 (w), 2019 (m), 1996 (s), 1978 (m), 1948 (mw, br), 1937 (mw, br), 1760 (w, br). Single crystals suitable for X-ray diffraction studies were obtained by slow cooling of a saturated MeOH/*i*-PrOH solution to −20 °C.

(21) (a) Coucouvanis, D. *ACS Symp. Ser.* **1988**, *372*, 390. (b) Al-Ahmad, S. A.; Salifoglou, A.; Kanatzidis, M. G.; Dunham, W. R.; Coucouvanis, D. *Inorg. Chem.* **1990**, *29*, 927. (c) Coucouvanis, D.; Salifoglou, A.; Kanatzidis, M. G.; Simopoulos, A.; Kostikas, A. *J. Am. Chem. Soc.* **1987**, *109*, 3807. (d) Salifoglou, A.; Kanatzidis, M. G.; Coucouvanis, D. *J. Chem. Soc., Chem. Commun.* **1986**, 559. (e) Kanatzidis, M. G.; Coucouvanis, D. *J. Am. Chem. Soc.* **1986**, *108*, 337. (f) Coucouvanis, D.; Kanatzidis, M. G. *J. Am. Chem. Soc.* **1985**, *107*, 5005. (g) Coucouvanis, D. *Acc. Chem. Res.* **1991**, *24*, 1.

(22) Coucouvanis, D.; Saleem, A.-A.; Salifoglou, A.; Dunham, W. R.; Sands, R. H. *Angew. Chem., Int. Ed. Engl.* **1988**, *27*, 1353.

(23) Seyferth, D.; Henderson, R. S.; Song, L. C. *Organometallics* **1982**, *1*, 125.

(24) (a) Nametkin, N. S.; Tyurin, V. D.; Aleksandrov, G. G.; Kuz'min, O. V.; Nekhaev, A. I.; Andrianov, V. G.; Mavlonov, M.; Struchkov, Yu. T. *Izv. Akad. Nauk SSSR, Ser. Khim.* **1979**, *28*, 1353. (b) Kovacs, J. A.; Bashkin, J. K.; Holm, R. H. *J. Am. Chem. Soc.* **1985**, *107*, 1784.

(25) (a) Lilley, G. L.; Sinn, E.; Averill, B. A. *Inorg. Chem.* **1986**, *25*, 1073. (b) Barber, D. E.; Bryan, R. F.; Averill, B. A. To be submitted for publication.

(26) Bose, K. S.; Lamberty, P. E.; Kovacs, J. A.; Sinn, E.; Averill, B. A. *Polyhedron* **1986**, *5*, 393.

(27) Eldredge, P. A.; Bryan, R. F.; Sinn, E.; Averill, B. A. *J. Am. Chem. Soc.* **1988**, *110*, 5573. A detailed analysis of the Mössbauer spectra of I is in progress.

(28) Bose, K. S.; Chmielewski, S. A.; Eldredge, P. A.; Sinn, E.; Averill, B. A. *J. Am. Chem. Soc.* **1989**, *111*, 8953.

(29) (a) Hieber, W.; Gruber, J. *Z. Anorg. Allg. Chem.* **1958**, *296*, 91. (b) Bogan, L. E., Jr.; Lesch, D. A.; Rauchfuss, T. B. *J. Organomet. Chem.* **1983**, *250*, 432.

(30) Bose, K. S.; Sinn, E.; Averill, B. A. *Organometallics* **1984**, *3*, 1126.

(31) Abel, E. W.; Butler, I. S.; Reid, J. G. *J. Chem. Soc.* **1963**, 2068.

(32) Burgmayer, S. J. N.; Templeton, J. L. *Inorg. Chem.* **1985**, *24*, 2224.

B. $(Et_4N)_2[MoFe_6S_6(CO)_{16}]$, $(Et_4N)_2$(I). To a green solution of 12.5 mmol of $[Fe_2S_2(CO)_6]^{2-}$ in 100 mL of THF (generated from 4.3 g (12.5 mmol) of $Fe_2S_2(CO)_6$ and 25 mL of 1.0 M $LiEt_3BH$ as described in part A above) at −78 °C was added via syringe a room-temperature solution of 4.2 g (5.9 mmol) of $(Et_4N)[Mo(CO)_4I_3]$ in 40 mL of THF. Immediate evolution of CO was observed. The brown reaction mixture was allowed to warm to room temperature, maintained at 45–50 °C in an oil bath for 3.5 h, and allowed to stand at room temperature overnight. The solvent was removed in vacuo at room temperature, the residue was dissolved in ca. 200 mL of MeOH, and the resulting brown solution was filtered. To the stirred filtrate was added 4 g (24 mmol) of $(Et_4N)Cl$ in 25 mL of MeOH; crystals were observed to form immediately. The mixture was stored at room temperature overnight, and the crystalline precipitate was collected by filtration, washed with 10 mL of MeOH, followed by 50 mL of Et_2O, and dried in vacuo. Yield: 36% (2.7 g). Anal. Calcd for $C_{33}H_{40}Fe_6MoN_2O_{16}S_6$: C, 28.83; H, 3.03; Fe, 25.16; Mo, 7.20; N, 2.10; S, 14.44. Found: C, 28.57; H, 3.04; Fe, 24.45; Mo, 7.06; N, 2.15; S, 14.69. IR (MeCN), cm^{-1} (ν(CO)): 2048 (vw), 2019 (m), 1997 (vs), 1978 (mw), 1947 (w, br), 1937 (sh), 1762 (w, br). Single crystals suitable for X-ray diffraction were obtained by slow cooling of a saturated solution in 4/1 *i*-PrOH/MeOH from room temperature to −20 °C.

C. $(Pr_4N)_2MoFe_4S_3(CO)_{14}$, $(Pr_4N)_2$(II). To the reddish mother liquor obtained after filtration of $(Et_4N)_2$(I) in part B above was added ca. 20 mL of *i*-PrOH, and the solution was cooled to −20 °C overnight. A small amount of solid that formed was removed by filtration, the filtrate was warmed to room temperature, 5 g (19 mmol) of $(Pr_4N)Br$ in a minimum volume of MeOH was added, and the solution was stored at −20 °C for several days. The crystalline solid was filtered out, washed with MeOH, and redissolved in a minimum amount of MeCN (ca. 30 mL). A solution of 2 g (7.5 mmol) of $(Pr_4N)Br$ in 120 mL of *i*-PrOH was added, the solution stored at −20 °C for several days, and the crystalline precipitate collected by filtration, washed with small portions of MeOH, and dried in vacuo. Yield: 23% (1.6 g). Anal. Calcd for $C_{38}H_{56}Fe_4MoN_2O_{14}S_3$: C, 38.67; H, 4.78; Fe, 18.93; Mo, 8.13; N, 2.37; S, 8.15. Found: C, 38.76; H, 4.81; Fe, 17.92; Mo, 7.94; N, 2.13; S, 8.51. IR (MeCN), cm^{-1} (ν(CO)): 2045 (w), 2011 (s), 2001 (s), 1969 (s), 1934 (m), 1921 (sh), 1830 (w, br), 1775 (w, br).

D. $(Ph_4As)_2[MoFe_4S_3(CO)_{13}(PEt_3)]$, $(Ph_4As)_2$(II-P). The Ph_4As^+ salt of II was isolated from the combined mother liquors obtained after filtration of $(Et_4N)_2$(I) from several preparations carried out as in part B above (containing $(Et_4N)_2$(II)) by addition of a solution of excess $(Ph_4As)Cl$ in *i*-PrOH to give a microcrystalline precipitate and a colorless supernatant. Recrystallization was accomplished by slow diffusion of *i*-PrOH into a concentrated MeCN solution of the product, resulting in long needles of $(Ph_4As)_2$(II) that were not suitable for crystallographic studies. IR (MeCN), cm^{-1} (ν(CO)): 2043 (m), 2007 (s), 1997 (s), 1966 (vs), 1933 (m), 1830 (w, br), 1774 (w, vbr).

A solution of 0.79 (0.5 mmol) of $(Ph_4As)_2$(II) and 230 μL (1.5 mmol) of Et_3P in ca. 70 mL of MeCN was maintained at 40 °C for 24 h; IR spectra of the dark orange solution indicated that the reaction was quantitative. The solvent was removed in vacuo, and X-ray-quality crystals were obtained by slow diffusion of *i*-PrOH into a concentrated MeCN solution of the product, followed by filtration, washing with *i*-PrOH, and drying in vacuo. Yield: 60% (0.50 g). Anal. Calcd for $C_{67}H_{55}As_2Fe_4MoO_{13}PS_3$: C, 48.34; H, 3.33; Fe, 13.42; Mo, 5.76; P, 1.86; S, 5.78. Found: C, 48.44; H, 3.12; Fe, 13.83; Mo, 5.45; P, 1.87; S, 6.07. IR (MeCN), cm^{-1} (ν(CO)): 2016 (w), 1993 (vs), 1962 (s), 1941 (w), 1930 (m), 1902 (sh), 1825 (w, vbr), 1766 (w, vbr).

E. $(Ph_4As)_2[Mo_2Fe_2S_2(CO)_{12}]$, $(Ph_4As)_2$(III). A solution of 0.50 g (1.5 mmol) of $[Fe_2S_2(CO)_6]$ was reduced to the dianion with 3.0 mL of $LiEt_3BH$ as described in part A above. Upon completion of the reduction, a solution of 0.72 g (1.5 mmol) of $Et_4N[Mo(CO)_5I]$ in 50 mL of THF was added dropwise. The reaction mixture was slowly brought to room temperature and then filtered, and the solvent was removed from the filtrate in vacuo. The resulting oil was dissolved in a 5% v/v CH_3CN/MeOH solution. A solution containing 1.0 g (4.8 mmol) of $(Et_4N)Br$, also in 5% v/v CH_3CN/MeOH, was added dropwise to the reaction mixture. When the mixture was cooled to −20 °C, the product precipitated as dark brown microcrystals that were isolated by filtration. Recrystallization was effected by dissolving the product in the 5% solvent, heating to 40 °C, and slowly cooling to −20 °C. Yield: 26% (0.37 g). Metathesis to the Ph_4As^+ salt was effected by ion-exchange chromatography. Approximately 20 g of DE 52 gel was washed three times with MeOH and transferred to a fritted column (25-mm diameter). A 0.28 M solution of HCl in MeOH was prepared by adding 7.0 mL of concentrated HCl to 300 mL of MeOH. The column was washed with approximately 90 mL of the 0.28 M HCl solution, rinsed with 90 mL of MeOH, and then equilibrated with 50 mL of a 50% v/v CH_3CN/MeOH solution. To the column was added 300 mg (0.31 mmol) of $(Et_4N)_2[Mo_2Fe_2S_2(CO)_{12}]$ dissolved in 30 mL of the 50% solution. The cluster was transferred to the column with 30 mL of 50% solution, at which point all of the cluster adhered to the gel. The column was washed with 100 mL of MeOH, and the cluster was eluted with 120 mL of a 0.15 M LiOMe/MeOH solution. After the volume of the eluant was reduced in vacuo to approximately 50 mL, a solution of 1.0 g (2.4 mmol) of $(Ph_4As)Cl$ in 50 mL of MeOH was added dropwise. A crystalline product began to form. Addition was stopped when the supernatant was colorless, and the product was isolated by filtration. Recrystallization was effected by dissolving the microcrystals in 70 mL of a 5% v/v CH_3CN/THF solution and layering with approximately 15 mL of hexane. Yield: 48% (0.22 g). Anal. Calcd for $C_{60}H_{40}As_2Fe_2Mo_2O_{12}S_2$: C, 49.01; H, 2.74; As, 10.19; Fe, 7.60; Mo, 13.05; S, 4.36. Found: C, 49.34; H, 2.84; As, 10.50; Fe, 7.75; Mo, 12.83; S, 4.36. IR (MeCN), cm^{-1} (ν(CO)): 2017 (w), 1970 (s), 1950 (s), 1931 (s), 1924 (s), 1852 (m, br), 1775 (mw, br).

F. $(Ph_4As)_2[MoFe_4S_3(CO)_{14}]$, $(Ph_4As)_2$(II) (from $[Mo(CO)_5I]^-$). The reaction of $[Fe_2S_2(CO)_6]^{2-}$ and $(Et_4N)[Mo(CO)_5I]$ was carried out exactly as described in part E above. After filtration of the reaction mixture, the solids were extracted with three 15-mL portions of THF. The combined filtrates were evaporated in vacuo, and the resulting oil was dissolved in 50 mL of MeOH. A solution of 0.91 g (2.2 mmol) of $(Ph_4As)Cl$ in 50 mL of MeOH was added dropwise, and the solution was stored at −20 °C for 12 h. The reddish brown crystalline precipitate was isolated by filtration, washed with MeOH, and dried in vacuo. The carbonyl region of the IR spectrum was identical with that of $(Pr_4N)_2$(II) prepared in part C above. Yield: 14% (0.31 g).

X-ray Analyses. Crystal data and details of data collection and refinement procedures are summarized in Table I for $(Ph_4As)_2[MoFe_6S_6(CO)_{16}]$ ($(Ph_4As)_2$(I)), $(Et_4N)_2[MoFe_6S_6(CO)_{16}]$ ($(Et_4N)_2$(I)), $(Ph_4As)_2[MoFe_4S_3(CO)_{13}(PEt_3)]$ ($(Ph_4As)_2$(II-P)), and $(Ph_4As)_2[Mo_2Fe_2S_2(CO)_{12}]$ ($(Ph_4As)_2$(III)). In addition, a data set was collected on a crystal of $(Pr_4N)_2[MoFe_4S_3(CO)_{14}]$ ($(Pr_4N)_2$(II)) and the structure solved, but relatively poor crystal quality and extreme disorder of the Pr_4N^+ cations precluded a high-resolution structure. The connectivity and general features of the structure of II were identical with those of II-P in the more accurate structure of the latter. In all four structures reported in this paper, the cations were crystallographically ordered with no anomalous features; hence, they will not be discussed further, although structural parameters are provided in the supplementary material.

$(Ph_4As)_2$(I). The structure was solved by using SHELXS-86,[33] and the core structure was confirmed independently by a Patterson map. The structure was refined to convergence $(\Delta/\sigma)_{max} < 0.10$ by using the block-diagonal, least-squares method. The atoms of the anion and the two As atoms were refined anisotropically, and no account was taken of the contributions of the H atoms. An empirical absorption correction[34] was applied to the observed structure amplitudes at the conclusion of the isotropic refinement. The maximum and minimum corrections were 0.42 and 1.58, which lowered R from 10.7% to 10.1% prior to anisotropic refinement.

$(Et_4N)_2$(I). Unit cell parameters were determined by least-squares refinement of the setting angles of 25 unique reflections. The data were corrected for Lp, absorption, and decay (8%) effects. All calculations were done by using the TEXSAN software package on a VAXstation II/RC computer. The positions of the metal and sulfur atoms were determined by using MULTAN. The remaining non-hydrogen atoms were located from difference Fourier maps. Full-matrix least-squares refinement was performed with anisotropic thermal parameters for all non-hydrogen atoms. The goodness-of-fit was 1.34. The final difference Fourier map was essentially featureless with the largest peak of 0.48 e/Å^3.

$(Ph_4As)_2$(II-P). The space group was unambiguously determined from systematic absences. The intensities of the reflections were corrected for a 4% linear decay in check reflection intensities and corrected empirically for absorption. The structure was solved by direct methods, and refined with anistropic thermal parameters for all non-hydrogen atoms with hydrogen atoms introduced at idealized positions.

$(Ph_4As)_2$(III). Space group symmetry required the molecule to be centrosymmetric, as confirmed by the analysis. The structure was refined to convergence $(\Delta/\sigma)_{max} < 0.10$ by using the block-diagonal, least-squares method. As with $(Ph_4As)_2$(I), an empirical absorption correction[34] was applied, with corrections ranging from 0.78 to 1.26, which lowered R from 16.4% to 14.9% prior to anisotropic refinement. All atoms except H were refined anisotropically, and H atoms were included in fixed

(33) Sheldrick, G. M. SHELXS-86, a Fortran program for the solution of crystal structures from diffraction data. University of Göttingen, Göttingen, BRD, 1986.
(34) Walker, N.; Stuart, D. *Acta Crystallogr., Sect. A.: Found. Crystallogr.* **1983**, *A39*, 158.

Table I. Crystal Data and Details of Data Collection and Refinement Procedures for $(Ph_4As)_2(I)$, $(Et_4N)_2(I)$, $(Ph_4As)_2(II\text{-}P)$, and $(Ph_4As)_2(III)$

	$(Ph_4As)_2(I)$	$(Et_4N)_2(I)$	$(Ph_4As)_2(II\text{-}P)$	$(Ph_4As)_2(III)$
formula	$C_{64}H_{40}As_2Fe_6MoO_{16}S_6$	$C_{32}H_{56}Fe_6MoN_2O_{16}S_6$	$C_{67}H_{55}As_2Fe_4MoO_{13}PS_3$	$C_{60}H_{40}As_2Fe_2Mo_2O_{12}S_2$
fw	1838.3	1348.2	1664	1470.5
space group	$P\bar{1}$ (No. 2)	$P2_1/c$ (No. 14)	$P2_1/c$ (No. 14)	$P2_1/m$ (No. 11)
cryst syst	triclinic	monoclinic	monoclinic	monoclinic
a, Å	12.473 (12)	19.275 (7)	18.124 (4)	11.938 (20)
b, Å	12.836 (13)	11.940 (3)	15.630 (3)	16.729 (30)
c, Å	22.360 (22)	20.975 (1)	24.665 (5)	15.694 (25)
α, deg	90.96 (2)			
β, deg	97.58 (2)	90.38 (4)	98.109 (2)	111.45 (50)
γ, deg	99.52 (2)			
V, Å^3	3497	4827	6917	2918
Z	2	4	4	4
cryst dimns, mm	0.20 × 0.20 × 0.35	0.30 × 0.30 × 0.40	0.15 × 0.45 × 0.40	0.25 × 0.30 × 0.30
color	black	black	dark red	brown/black
d(calc), g/cm^3	1.48	1.85	1.597	1.67
temp, °C	20	25	23	20
diffractometer	Nicolet P3m	Enraf-Nonius CAD 4	Nicolet R3m	Nicolet P3m
radiation	Mo Kα	Mo Kα	Mo Kα	Cu Kα
monochromator	graphite	graphite	graphite	graphite
μ, cm^{-1}	25.6	23.56	21.07	127
scan technique	θ–2θ	θ–2θ	Wyckoff	θ–2θ
scan range, deg	3.5–60	1–46	4–42	2–114
data collected: h, k, l	+13, ±15, +25 to −26	+21, +12, ±21	±19, +16, +25	+12, +18, +15 to −16
no. of indep reflections	14563	6664	7514	3947
no. of unique data used with $I > n\sigma(I)$	9146	3872	3874	3182
n	2.5	3	5	3
solution program	SHELXS-86	MULTAN	SHELXTL(5.1)	SHELXS-86
R	8.3	3.8	6.3	6.2
R_w	9.4	4.8	6.3	5.8

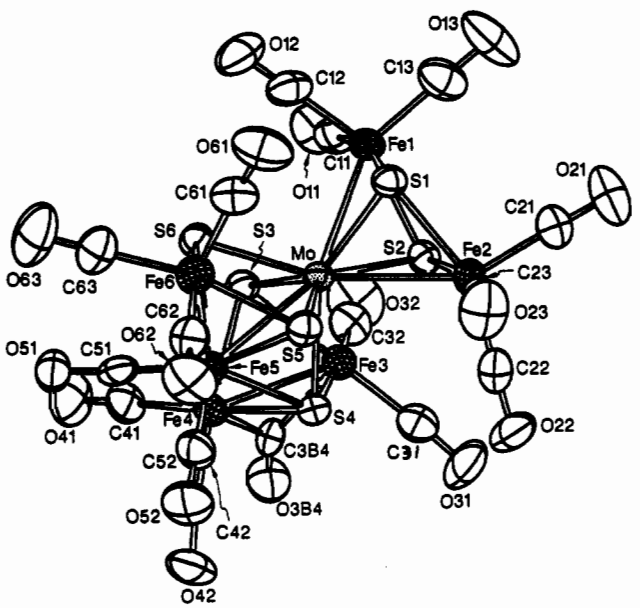

Figure 1. ORTEP drawing of the $[MoFe_6S_6(CO)_{16}]^{2-}$ ion in $(Et_4N)_2(I)$, showing the atomic labeling scheme.

positions with isotropic B values fixed at B_{eq} + 1 Å^2 for the carbon of attachment.

Results and Discussion

Description of the Structure of the $[MoFe_6S_6(CO)_{16}]^{2-}$ Ion (I). Because of the unexpectedly low-symmetry structure of I in the Ph_4As^+ salt previously reported,[27] the structure of the Et_4N^+ salt of I was also determined. Selected distances and angles for the anions are given in Table II for both salts. A view of the overall structure of I is shown in Figure 1 along with the atomic labeling scheme, and a stereoview is given in Figure 2, while the structure of the $MoFe_6S_6$ core is shown in Figure 3. In the discussion that follows, metrical parameters cited are those for the more precise structure of the Et_4N^+ salt of I; all structural parameters of the anions are essentially identical (within two standard deviations) for both salts, however.

Anion I has no crystallographically imposed symmetry, and in fact does not even approximate a symmetry higher than C_1. The structure is based on a distorted trigonal-prismatic MoS_6 unit, whose dimensions are shown in Figure 4a, while a view down the pseudo-3-fold axis of the MoS_6 unit is given in Figure 4b. Sulfur atoms S1, S5, S6 and S2, S3, S4 form the top and bottom triangles, respectively, which are severely distorted from equilateral (angles range from 49.57 (6) to 70.96 (8)°; S---S distances, from 2.902 (3) to 3.605 (3) Å). The most acute angles of each triangle (S6–S1–S5 and S3–S2–S4) are approximately eclipsed. In addition to the distortions within each S_3 triangle, the triangles are not precisely parallel, with intertriangle S–S distances ranging from 2.949 (3) to 3.080 (3) Å. The two triangles are rotated away from an eclipsed orientation by a twist angle of ca. 13°. As a

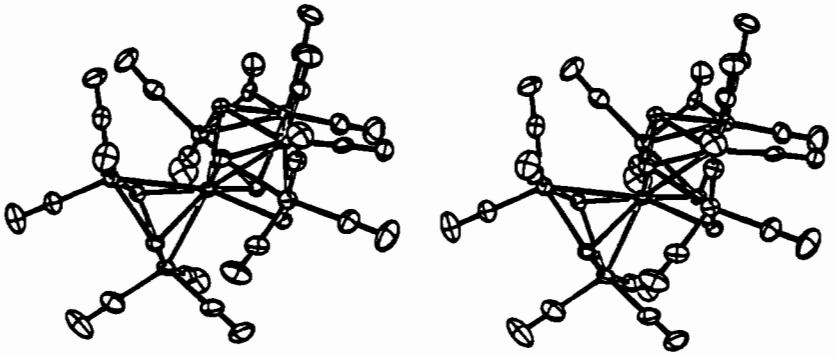

Figure 2. Stereoview of the $[MoFe_6S_6(CO)_{16}]^{2-}$ ion in $(Et_4N)_2(I)$ in the same orientation as in Figure 1.

Table II. Interatomic Distances (Å) and Angles (deg) in the Core of the $[MoFe_6S_6(CO)_{16}]^{2-}$ Anion

Distances

	$(NEt_4)^+$	$(AsPh_4)^+$		$(NEt_4)^+$	$(AsPh_4)^+$		$(NEt_4)^+$	$(AsPh_4)^+$		$(NEt_4)^+$	$(AsPh_4)^+$
Mo-S1	2.369 (2)	2.360 (5)	Mo-Fe6	3.639 (2)	3.618 (4)	Fe4-S3	2.311 (3)	2.300 (6)	S1-S2	2.948 (3)	2.952 (7)
Mo-S2	2.442 (2)	2.441 (5)	Fe1-S1	2.259 (3)	2.262 (6)	Fe4-S4	2.294 (3)	2.304 (6)	S1-S5	3.284 (3)	3.256 (7)
Mo-S3	2.493 (2)	2.478 (6)	Fe1-S2	2.282 (3)	2.284 (7)	Fe4-Fe5	2.744 (2)	2.749 (4)	S1-S6	3.604 (3)	3.595 (8)
Mo-S4	2.396 (2)	2.433 (7)	Fe1-Fe2	3.414 (2)	3.419 (4)	Fe5-S3	3.405 (3)	3.422 (7)	S2-S3	3.332 (3)	3.307 (8)
Mo-S5	2.470 (2)	2.462 (5)	Fe2-S1	2.265 (3)	2.262 (6)	Fe5-S4	2.348 (3)	2.346 (6)	S2-S4	3.570 (3)	3.636 (7)
Mo-S6	2.387 (2)	2.389 (6)	Fe2-S2	2.272 (3)	2.273 (6)	Fe5-S5	2.241 (3)	2.235 (6)	S3-S4	3.099 (3)	3.114 (6)
Mo-Fe1	2.735 (2)	2.741 (5)	Fe3-S2	2.628 (3)	2.649 (6)	Fe5-S6	2.288 (3)	2.285 (6)	S3-S6	3.080 (3)	3.026 (6)
Mo-Fe2	2.763 (2)	2.766 (5)	Fe3-S3	2.228 (3)	2.215 (6)	Fe5-Fe6	2.583 (2)	2.582 (6)	S4-S5	2.976 (3)	3.017 (7)
Mo-Fe3	2.983 (2)	2.964 (5)	Fe3-S4	2.423 (3)	2.418 (5)	Fe6-S5	2.247 (3)	2.248 (6)	S4-S6	3.829 (3)	3.832 (10)
Mo-Fe4	3.491 (2)	3.484 (6)	Fe3-Fe4	2.578 (2)	2.581 (5)	Fe6-S6	2.232 (3)	2.230 (6)	S5-S6	2.902 (3)	2.918 (6)
Mo-Fe5	2.676 (2)	2.678 (3)									

Angles

	$(NEt_4)^+$	$(AsPh_4)^+$		$(NEt_4)^+$	$(AsPh_4)^+$		$(NEt_4)^+$	$(AsPh_4)^+$
S1-Mo-S2	75.6 (1)	75.9 (2)	S6-Mo-Fe5	53.4 (1)	53.2 (2)	S3-Fe4-S5	84.6 (1)	85.1 (2)
S1-Mo-S3	135.0 (1)	133.9 (2)	Fe1-Mo-Fe2	76.8 (1)	76.7 (1)	S3-Fe4-Fe3	53.9 (1)	53.6 (2)
S1-Mo-S4	142.3 (1)	143.9 (2)	Fe1-Mo-Fe5	152.5 (1)	151.5 (2)	S3-Fe4-Fe5	84.2 (1)	84.8 (2)
S1-Mo-S5	85.5 (1)	84.9 (2)	Fe2-Mo-Fe5	128.8 (1)	129.5 (1)	S4-Fe4-Fe3	59.3 (1)	59.0 (2)
S1-Mo-S6	98.6 (1)	98.4 (2)	S1-Fe1-S2	81.0 (1)	81.0 (2)	S4-Fe4-Fe5	54.7 (1)	54.5 (2)
S1-Mo-Fe1	52.0 (1)	52.0 (2)	S1-Fe1-Mo	55.7 (1)	55.3 (2)	Fe3-Fe4-Fe5	102.9 (6)	102.2 (2)
S1-Mo-Fe2	51.7 (1)	52.0 (2)	S1-Fe1-Fe2	41.1 (1)	41.3 (2)	S4-Fe5-S5	80.8 (1)	82.3 (2)
S2-Mo-S3	84.9 (1)	84.5 (2)	S2-Fe1-Mo	57.4 (1)	57.3 (2)	S4-Fe5-S6	111.4 (1)	111.6 (2)
S2-Mo-S4	95.1 (1)	96.5 (2)	S2-Fe1-Fe2	41.3 (1)	41.3 (2)	S5-Fe5-S6	79.7 (1)	80.4 (2)
S2-Mo-S5	134.6 (1)	135.5 (2)	Mo-Fe1-Fe2	52.0 (1)	52.0 (1)	S4-Fe5-Mo	56.5 (1)	57.4 (2)
S2-Mo-S6	149.3 (1)	147.7 (2)	S1-Fe2-S2	81.1 (1)	81.0 (2)	S4-Fe5-Fe4	52.9 (1)	53.1 (2)
S2-Mo-Fe1	51.9 (1)	51.9 (2)	S1-Fe2-Mo	55.2 (1)	54.8 (2)	S4-Fe5-Fe6	134.1 (1)	135.4 (2)
S2-Mo-Fe2	51.3 (1)	51.3 (2)	S1-Fe2-Fe1	41.0 (1)	41.0 (2)	S5-Fe5-Mo	59.5 (1)	59.3 (2)
S3-Mo-S4	78.6 (1)	78.8 (2)	S2-Fe2-Mo	57.0 (1)	56.9 (2)	S5-Fe5-Fe4	131.2 (1)	132.0 (2)
S3-Mo-S5	133.8 (1)	134.4 (2)	S2-Fe2-Fe1	41.6 (1)	41.5 (2)	S5-Fe5-Fe6	55.0 (1)	55.1 (2)
S3-Mo-S6	78.3 (1)	76.9 (2)	Mo-Fe2-Fe1	51.3 (1)	51.3 (1)	S6-Fe5-Mo	56.8 (1)	56.9 (2)
S3-Mo-Fe5	82.3 (1)	83.1 (2)	S2-Fe3-S3	86.2 (1)	85.2 (2)	S6-Fe5-Fe4	101.6 (1)	98.7 (2)
S4-Mo-S5	75.4 (1)	76.1 (2)	S3-Fe3-S4	83.4 (1)	84.4 (2)	S6-Fe5-Fe6	54.2 (1)	54.1 (2)
S4-Mo-S6	106.4 (1)	105.3 (2)	S2-Fe3-S4	89.9 (1)	91.6 (2)	Fe6-Fe5-Mo	87.6 (1)	86.9 (2)
S4-Mo-Fe5	54.8 (1)	54.4 (2)	S2-Fe3-Fe4	128.4 (1)	128.4 (2)	Fe4-Fe5-Fe6	155.4 (1)	152.5 (1)
S5-Mo-S6	73.4 (1)	73.9 (2)	S3-Fe3-Fe4	56.9 (1)	56.7 (2)	Mo-Fe5-Fe4	80.2 (1)	79.9 (2)
S5-Mo-Fe5	51.4 (1)	51.4 (2)	S4-Fe3-Fe4	54.5 (1)	54.8 (2)	S5-Fe6-S6	80.8 (1)	80.4 (2)

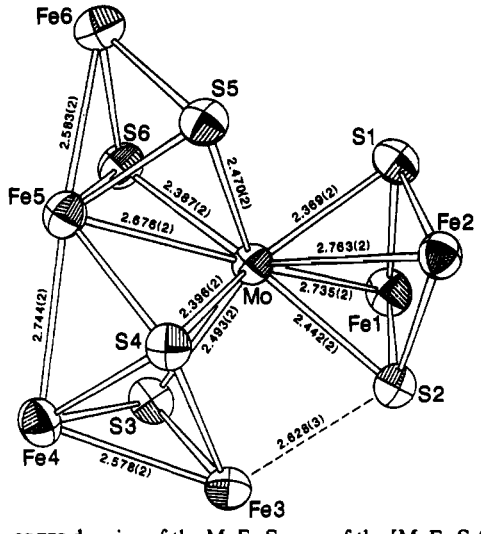

Figure 3. ORTEP drawing of the $MoFe_6S_6$ core of the $[MoFe_6S_6(CO)_{16}]^{2-}$ ion (I), showing selected interatomic distances.

result, the S_4 faces of the trigonal prism are not perfectly planar, but rather are rhombs puckered about a diagonal of each face (as is clearly shown in Figure 4b). The deviation from planarity within the S_4 faces ranges from 0.09 Å for S1–S2–S4–S5 to 0.23 Å for S3–S4–S5–S6.

The six iron atoms are arranged about a pseudo-2-fold axis of the trigonal prism (that containing the midpoint of the S1–S2 edge and the center of the S3–S4–S5–S6 rhomb) in groups of two and four. In one direction along this axis is an essentially isolated $Fe_2S_2(CO)_6$ unit, containing Fe1, Fe2, S1, and S2, with a relatively long (2.628 (3) Å) bond linking Fe3 and S2. As expected, the bond distances from Fe1 and Fe2 to the quadruply bridging sulfide (S2) are significantly longer (0.07 to 0.20 Å) than are those to the triply bridging sulfide (S1). The most notable features of the coordinated $Fe_2S_2(CO)_6$ group are the long Fe1–Fe2 distance (3.419 (2) Å) (vs 2.55 and 2.54 Å for the parent $Fe_2S_2(CO)_6$[35] and for $Fe_2(SEt)_2(CO)_6$,[36] respectively), with an accompanying severe distortion of the Fe_2S_2 core toward planarity (all atoms are within 0.22 Å of being coplanar), and the short Mo–Fe1 and Mo–Fe2 distances (2.735 (2) and 2.763 (2) Å, respectively). The latter are well within the range of distances reported for other synthetic Mo–Fe–S clusters of the "cubane" and "linear" varieties,[19] which are generally interpreted as indicating some degree of net Mo–Fe bonding interaction. It thus appears as if the Fe–Fe bond of the parent $Fe_2S_2(CO)_6$ unit has been replaced by two new Mo–Fe bonds.

In the other direction along the pseudo-2-fold axis of the trigonal prism is a zigzag chain of four iron atoms (Fe3–Fe6) spanning the S3–S4–S5–S6 rhomb and connected to the rest of the molecule only via the aforementioned long Fe3–S2 interaction. The tetrairon chain clearly results from partial fusion of two $Fe_2S_2(CO)_6$ units attached to Mo, via formation of a new Fe5–S4 bond at 2.348 (3) Å, resulting in a quadruply bridging sulfide (S4), and an Fe4–Fe5 bond at 2.744 (2) Å. The latter is accompanied by a lengthening of the Fe–Fe bonds in the $Fe_2S_2(CO)_6$ units by ca. 0.1 Å vs values typically observed for coordinated $Fe_2S_2(CO)_6$ units,[24-26] together with formation of a bond between Mo and Fe5 (2.676 (2) Å). This partial fusion is accompanied by loss of a CO ligand from Fe5 and Fe4 and formation of a bridging CO between Fe3 and Fe4. Thus, new Fe–Fe and Mo–Fe bonds have apparently been formed within the $MoFe_4$ unit at the expense of some net Fe–Fe bonding within the $Fe_2S_2(CO)_6$ units.

Salient points regarding the structure of I include the following.

(35) Wei, C. H.; Dahl, L. F. *Inorg. Chem.* **1965**, *4*, 1.
(36) Dahl, L. F.; Wei, C. H. *Inorg. Chem.* **1963**, *2*, 328.

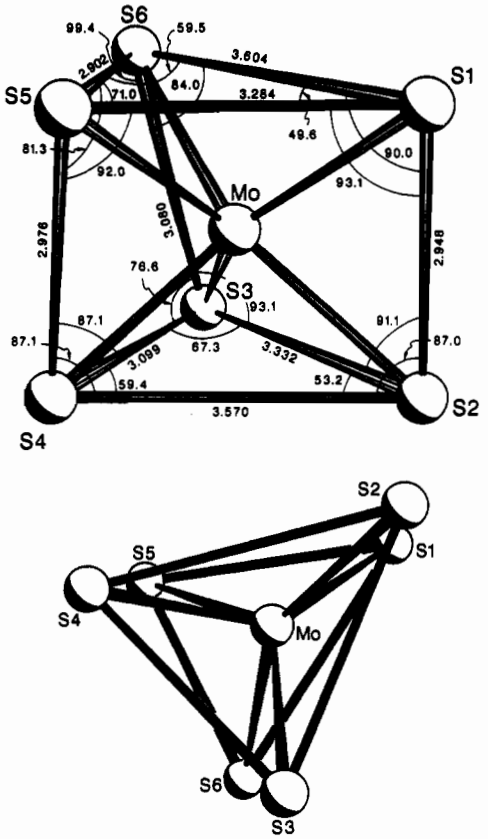

Figure 4. (a) Top: View of the MoS_6 core of the $[MoFe_6S_6(CO)_{16}]^{2-}$ ion (I), showing the dimensions of the distorted trigonal prism. (b) Bottom: View down the pseudo-3-fold axis of the distorted trigonal prism.

(i) The $MoFe_6S_6$ core stoichiometry constitutes the closest approximation yet in a synthetic complex to the composition of FeMo-co. Cluster I is the first synthetic species containing a single molybdenum to exceed the 4/1 Fe/Mo ratio reported for the single cubane derivative $[MoFe_4S_4(SEt)_3(cat)_3]^{3-}$ containing an appended tris(catecholato)iron unit[37] and the 5/1 Fe/Mo ratio reported for the $[MoOFe_5S_6(CO)_{12}]^{2-}$ cluster containing a molybdenum–oxo group.[26] (ii) The Mo–Fe distances divide into two sets, three at ca. 2.70 ± 0.06 Å and three in the 3.0–3.6-Å range. The former arise from a previously unexpected tendency of low-valent molybdenum (oxidation states +2 and 0) to form new Mo–Fe bonds at the expense of Fe–Fe bonds during the reaction with $[Fe_2S_2(CO)_6]^{2-}$. (For additional examples, see the structures of clusters II-P and III below.) As a result, the Mo–Fe distance distribution in I is similar to that observed for FeMo-co, for which EXAFS measurements[11,12] have indicated the presence of 3 ± 1 iron neighbors to molybdenum at ca. 2.7 Å, with the rest of the iron atoms presumably too distant to be detected. It should be noted, however, that recent Fe EXAFS studies of isolated FeMo-co have also provided evidence for a 3.68-Å Fe–Fe or Fe–Mo interaction.[12b] (iii) The Mo–S distances also divide into two sets of three, at 2.384 (4) Å (S1, S4, S6) and 2.468 (4) Å (S2, S3, S5). The sulfur atoms at both shorter and longer distances are each arranged in a roughly planar fashion around the molybdenum, with a dihedral angle of 83.7° between the two S_3 planes. (iv) The average Mo–S distance of 2.43 Å is significantly longer than those reported for either the "linear" MoS_2Fe clusters (ca. 2.20 Å)[19a–c,e] or the "cubane" $MoFe_3S_4$ clusters (ca. 2.35 Å),[19a,b,d] which have formal molybdenum oxidation states of +6 and +3 or +4, respectively, and significantly shorter than those reported for the doubly Mo(CO)$_3$-capped hexamers (2.58–2.65 Å),[21] which have formal molybdenum oxidation states of zero. Although a variety of structural constraints are present in these systems that might result in anomalous bond distances, the available structural data on other

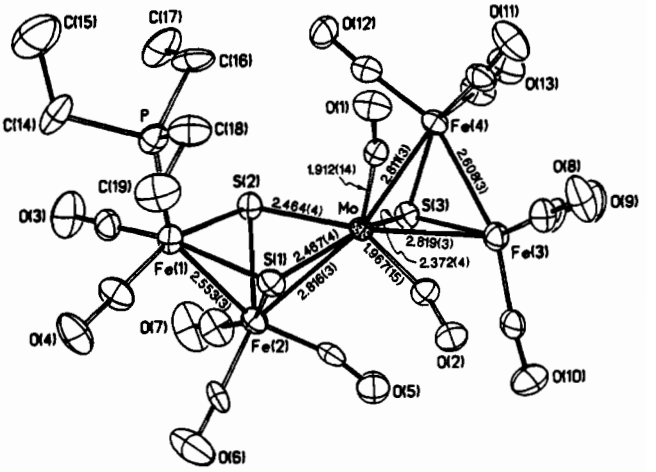

Figure 5. ORTEP drawing of the $[MoFe_4S_3(CO)_{13}(PEt)_3]^{2-}$ ion (II-P), showing the atomic labeling scheme and selected interatomic distances.

Mo–Fe–S clusters are most consistent with a molybdenum oxidation state of ca. +2 in cluster I. Molybdenum EXAFS studies on FeMo-co and its MoFe-protein complex reveal an average Mo–S distance of 2.37 Å,[11] consistent with a higher formal oxidation state for molybdenum in FeMo-co than in I. (v) The dianonic nature of cluster I indicates that a $2e^-$ oxidation has occurred during its synthesis, inasmuch as simple addition of three $[Fe_2S_2(CO)_6]^{2-}$ units to Mo(II) should result in a tetraanion. If conclusion iv regarding the presence of Mo(II) in I is correct, then this implies that the oxidation is centered on the iron atoms, as is supported by preliminary Mössbauer data presented previously.[27] The presence of CO ligands on the iron atoms is consistent with a relatively low Fe oxidation state, but the paucity of appropriate CO–Fe–S complexes with well-defined Fe oxidation states and the presence of extensive metal–metal bonding in I make this point difficult to assess by examining Fe–S or Fe–CO distances. (vi) As a result of the presence of both triply and quadruply bridging sulfides together with Mo–Fe bonds, cluster I has an unusually low symmetry structure that appears to be the result of electronic considerations rather than, e.g., crystal packing effects. This is in distinct contrast to other synthetic Mo–Fe–S clusters prepared to date, which typically have either crystallographically imposed or effective higher symmetry, typically a 3-fold axis or mirror plane. It should also be noted that all of the structures proposed to date for FeMo-co possess intrinsically high symmetry as well.[19a,b,26,38] The possible importance of a low-symmetry structure such as that of I is indicated by recent ENDOR results[10a] that were interpreted as demonstrating intrinsically inequivalent iron sites in both MoFe-protein-bound FeMo-co and isolated FeMo-co in NMF. This conclusion has been questioned by others, however, on the basis of Mössbauer spectra of FeMo-co demonstrating equivalent iron sites[9c] and on the basis of the general argument that inequivalent hyperfine parameters may result from a particular spin-coupling model and need not reflect significant chemical differences at the iron sites.[9c] (vii) As a result of the formation of three Mo–Fe bonds in addition to the six sulfur atoms provided by the $Fe_2S_2(CO)_6$ units, the molybdenum atom in I is effectively nine-coordinate, utilizing all available valence orbitals. This is also true of all other previously reported Mo–Fe–S clusters containing molybdenum in intermediate oxidation states (e.g., the $MoFe_3S_4$ "cubane" clusters,[19a] for which the evidence for direct Mo–Fe bonding is less compelling) and represents a potentially important point for FeMo-co structure that has not been previously recognized.

Description of the Structure of the $[MoFe_4S_3(CO)_{13}(PEt_3)]^{2-}$ Ion (II-P). A view of the cluster anion II-P is shown in Figure 5, and selected distances and angles are given in Table III. As is the case with I, cluster II-P possesses no crystallographically

(37) Wolf, T. E.; Berg, J. M.; Holm, R. H. *Inorg. Chem.* **1981**, *20*, 174.

(38) (a) Holm, R. H. *Chem. Soc. Rev.* **1982**, *10*, 455. (b) Coucouvanis, D.; Challen, P. R.; Koo, S.-M.; Davis, W. M.; Butler, W.; Dunham, W. R. *Inorg. Chem.* **1989**, *28*, 4183.

Table III. Interatomic Distances (Å) and Angles (deg) in $[MoFe_4S_3(CO)_{13}(PEt_3)]^{2-}$ Anion

Distances			
Mo–Fe2	2.816 (3)	Mo–Fe3	2.819 (3)
Mo–Fe4	2.811 (3)	Mo–S1	2.467 (4)
Mo–S2	2.464 (4)	Mo–S3	2.372 (4)
Mo–C1	1.912 (14)	Mo–C2	1.967 (15)
Fe1–Fe2	2.553 (3)	Fe1–S1	2.274 (5)
Fe1–S2	2.275 (4)	Fe1–P	2.188 (5)
Fe1–C3	1.748 (16)	Fe1–C4	1.721 (16)
Fe2–S1	2.286 (4)	Fe2–S2	2.282 (5)
Fe2–C5	1.756 (19)	Fe2–C6	1.757 (18)
Fe2–C7	1.756 (18)	Fe3–Fe4	2.608 (3)
Fe3–S3	2.207 (5)	Fe3–C8	1.723 (16)
Fe3–C9	1.759 (18)	Fe3–C10	1.766 (18)
Fe4–S3	2.217 (5)	Fe4–C11	1.760 (16)
Fe4–C12	1.755 (16)	Fe4–C13	1.742 (16)
O1–C1	1.185 (17)	O2–C2	1.160 (18)
O3–C3	1.167 (20)	O4–C4	1.169 (20)
O5–C5	1.183 (24)	O6–C6	1.128 (23)
O7–C7	1.150 (23)	O8–C8	1.173 (20)
O9–C9	1.158 (22)	O10–C10	1.150 (22)
O11–C11	1.177 (20)	O12–C12	1.160 (20)
O13–C13	1.178 (20)		
Angles			
Fe2–Mo–Fe3	128.0 (1)	Fe2–Mo–Fe4	143.0 (1)
Fe3–Mo–Fe4	55.2 (1)	Fe2–Mo–S1	50.8 (1)
Fe3–Mo–S1	143.9 (1)	Fe4–Mo–S1	153.3 (1)
Fe2–Mo–S2	50.7 (1)	Fe3–Mo–S2	138.7 (1)
Fe4–Mo–S2	100.5 (1)	S1–Mo–S2	73.0 (1)
Fe2–Mo–S3	101.2 (1)	Fe3–Mo–S3	49.4 (1)
Fe4–Mo–S3	49.8 (1)	S1–Mo–S3	152.0 (1)
S2–Mo–S3	89.3 (1)	Fe2–Mo–C1	135.2 (4)
Fe3–Mo–C1	95.9 (4)	Fe4–Mo–C1	66.6 (4)
S1–Mo–C1	89.4 (4)	S2–Mo–C1	103.9 (4)
S3–Mo–C1	116.3 (4)	Fe2–Mo–C2	100.4 (4)
Fe3–Mo–C2	63.1 (4)	Fe4–Mo–C2	109.6 (4)
S1–Mo–C2	81.1 (4)	S2–Mo–C2	149.7 (5)
S3–Mo–C2	107.6 (4)	C1–Mo–C2	91.1 (6)
Fe2–Fe1–S1	56.2 (1)	Fe2–Fe1–S2	56.1 (1)
S1–Fe1–S2	80.2 (2)	Mo–Fe2–Fe1	87.1 (1)
Mo–Fe2–S1	56.7 (1)	Fe1–Fe2–S1	55.7 (1)
Mo–Fe2–S2	56.6 (1)	Fe1–Fe2–S2	55.8 (1)
S1–Fe2–S2	79.8 (2)	Mo–Fe3–Fe4	62.3 (1)
Mo–Fe3–S3	54.7 (1)	Fe4–Fe3–S3	54.1 (1)
Mo–Fe4–Fe3	62.6 (1)	Mo–Fe4–S3	54.8 (1)
Fe3–Fe4–S3	53.7 (1)	Mo–S1–Fe1	102.6 (2)
Mo–S1–Fe2	72.6 (1)	Fe1–S1–Fe2	68.1 (1)
Mo–S2–Fe1	102.7 (1)	Mo–S2–Fe2	72.7 (1)
Fe1–S2–Fe2	68.1 (1)	Mo–S3–Fe3	75.9 (1)
Mo–S3–Fe4	75.5 (1)	Fe3–S3–Fe4	72.2 (1)
Mo–C1–O1	166.7 (12)	Mo–C2–O2	165.2 (13)
Fe1–C3–O3	178.8 (16)	Fe1–C4–O4	175.6 (14)
Fe2–C5–O5	165.7 (18)	Fe2–C6–O6	178.2 (16)
Fe2–C7–O7	174.3 (18)	Fe3–C8–O8	175.7 (14)
Fe3–C9–O9	179.8 (21)	Fe3–C10–O10	173.2 (14)
Fe4–C11–O11	174.7 (15)	Fe4–C12–O12	176.8 (14)
Fe4–C13–O13	175.1 (15)		

imposed symmetry and approximates no symmetry higher than C_1. Ignoring short Mo–Fe contacts for the moment, the coordination about the molybdenum approximates square pyramidal, with Mo-C1 defining the axial position at angles of 89.4 (4), 91.1 (6), 103.9 (4), and 116.3 (4)° to the basal atoms. Within the basal plane, the S1–Mo–S3 and S2–Mo–C2 angles are 152.0 (1) and 149.7 (5)°, respectively. The axial Mo–C1 bond is ca. 0.05 Å shorter than the basal Mo–C2 bond as well. The four iron atoms are disposed about the molybdenum in pairs, resulting in the presence of a triangular $MoFe_2$ unit containing a single μ_3-sulfide (S3) and an asymmetrically coordinated $Fe_2S_2(CO)_5(PEt_3)$ unit containing two μ_3-sulfides. The $(\mu_3\text{-S})MoFe_2$ unit contains two Mo–Fe bonds (Mo–Fe_{av} = 2.815 Å), with an Fe–Fe bond that is ca. 0.05 Å longer than that in the parent $Fe_2S_2(CO)_6$,[35] once again suggesting that Mo–Fe bonds are formed at the expense of some net Fe–Fe bonding. The Mo–Fe3–Fe4 triangle is twisted by a dihedral angle of 133° to the Mo–S1–S2–Fe1 plane (actually a rhomb puckered about the S---S axis by ca. 0.1 Å), with S3 and Fe2 1.62 and 1.84 Å above the former and below the latter, respectively. A single PEt_3 substituent on the only iron atom not bonded to molybdenum completes the coordination.

Table IV. Interatomic Distances (Å) and Angles (deg) in the $[Mo_2Fe_2S_2(CO)_{12}]^{2-}$ Anion

Distances			
Mo–Mo′	4.104 (2)	Fe–C5	1.741 (13)
Mo–Fe	2.785 (6)	Fe–C6	1.735 (11)
Mo–Fe′	2.696 (6)	S–S′	2.986 (18)
Mo–S	2.531 (5)	C1–O1	1.135 (15)
Mo–S′	2.545 (8)	C2–O2	1.150 (13)
Mo–C1	2.040 (13)	C3–O3	1.142 (12)
Mo–C2	1.901 (13)	C4–O4	1.184 (11)
Mo–C3	1.909 (10)	C5–O5	1.153 (15)
Mo–C4	2.234 (10)	C6–O6	1.180 (13)
Fe–S	2.344 (7)	Fe–Fe′	3.634 (6)
Fe–S′	2.359 (6)	Fe–C1′	2.833 (14)
Fe–C4	1.996 (10)		
Angles			
Fe–Mo–Fe′	83.0 (2)	Mo–Fe–S	58.4 (1)
Fe–Mo–S	52.3 (2)	Mo–Fe–S′	58.6 (2)
Fe–Mo–S′	52.1 (3)	Mo–Fe–C4	52.6 (3)
Fe–Mo–C1	155.0 (4)	Mo–Fe–C5	122.3 (4)
Fe–Mo–C2	114.7 (3)	Mo–Fe–C6	124.8 (6)
Fe–Mo–C3	126.1 (4)	Mo′–Fe–S	60.2 (2)
Fe–Mo–C4	128.2 (3)	Mo′–Fe–S′	59.6 (2)
Fe′–Mo–S	53.5 (2)	Mo′–Fe–C4	149.4 (3)
Fe′–Mo–S′	53.1 (1)	Mo′–Fe–C5	113.0 (5)
Fe′–Mo–C1	72.0 (4)	Mo′–Fe–C6	108.2 (4)
Fe′–Mo–C2	128.1 (4)	S–Fe–S′	78.8 (4)
Fe′–Mo–C3	126.1 (4)	S–Fe–C4	95.6 (3)
Fe′–Mo–C4	128.2 (3)	S–Fe–C5	172.6 (4)
S–Mo–S′	72.1 (5)	S–Fe–C6	93.1 (5)
S–Mo–C1	110.1 (4)	S′–Fe–C4	100.0 (4)
S–Mo–C2	98.0 (5)	S′–Fe–C5	95.3 (5)
S–Mo–C3	161.7 (3)	S′–Fe–C6	167.6 (4)
S–Mo–C4	85.0 (3)	C4–Fe–C5	89.8 (5)
S′–Mo–C1	108.8 (4)	C4–Fe–C6	90.3 (5)
S′–Mo–C2	166.7 (3)	C5–Fe–C6	91.9 (6)
S′–Mo–C3	93.4 (6)	Mo–S–Mo′	107.9 (1)
S′–Mo–C4	88.4 (3)	Mo–S–Fe	69.6 (2)
C1–Mo–C2	82.6 (5)	Mo–S–Fe′	66.8 (1)
C1–Mo–C3	84.7 (5)	Mo′–S–Fe	66.8 (3)
C1–Mo–C4	159.7 (4)	Mo′–S–Fe′	69.1 (3)
C2–Mo–C3	94.4 (6)	Fe–S–Fe′	101.2 (4)
C2–Mo–C4	81.9 (4)	Fe–C4–Mo	82.1 (4)
C3–Mo–C4	83.6 (4)	Fe–C4–O4	138.8 (8)
Mo–Fe–Mo′	97.0 (2)	Mo–C4–O4	139.1 (7)

The most important features of the structure are the following. (i) One of the sulfur atoms of an $[Fe_2S_2(CO)_6]^{2-}$ unit has been lost during the cluster assembly reaction, leading to the monobridged $(\mu_3\text{-S})MoFe_2$ unit. (ii) The coordinated $Fe_2S_2(CO)_5(PEt_3)$ unit exhibits an Mo–Fe bonding interaction at 2.816 Å, with a corresponding increase of ca. 0.1 Å in the Fe–Fe bond length vs that normally observed in $Fe_2S_2(CO)_6$ units coordinated to a metal ion.[24-26] This asymmetric coordination mode has been previously observed only in the $MoFe_5S_6(CO)_6(PEt_3)_3$ "capped cubane" derivative.[28] (iii) The average Mo–S distance is 2.43 Å, the same as that in cluster I, suggesting a formal oxidation state of +2 for the molybdenum. This is consistent with elimination of the missing sulfur atom as elemental sulfur. (iv) As a result of the formation of three Mo–Fe bonds, the molybdenum atom in II-P is formally eight-coordinate, although nine-coordination might be expected for a Mo(II)-based cluster. Cluster II-P is also the only structurally characterized such cluster with π-acid ligands on molybdenum, and these may well be responsible for the apparently anomalous behavior.

Description of the Structure of the $[Mo_2Fe_2S_2(CO)_{12}]^{2-}$ Ion (III). A view of cluster anion III is shown in Figure 6, and selected distances and angles are given in Table IV. The cluster comprises a planar array of two molybdenum and two iron atoms, placed at opposite vertices of a regular parallelogram, with a single quadruply bridging sulfur atom above and below the plane; a center of symmetry is crystallographically required. As a result, the six atoms of the $Mo_2Fe_2S_2$ core form a distorted octahedron.

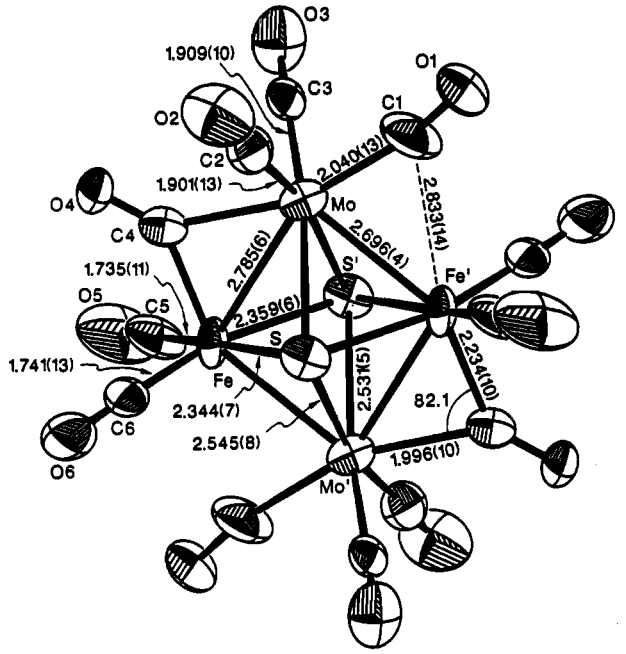

Figure 6. ORTEP drawing of the $[Mo_2Fe_2S_2(CO)_{12}]^{2-}$ ion (III), showing the atomic labeling scheme and selected interatomic distances.

The molybdenum atom is coordinated by three terminal CO's, and the iron atom by two, with a bridging CO between the iron and molybdenum. In addition, there appears to be a weak interaction between one of the carbonyls on molybdenum and the iron opposite the bridging CO, as evidenced by a short (2.833 (14) Å) Fe1–C1 distance and a significant bending of the oxygen atom of the carbonyl away from the iron (Mo–C1–O1 ≈ 170°). Significant features of the structure of III include the following. (i) The $Mo_2Fe_2S_2$ core stoichiometry clearly indicates that III arises from reaction of two $[Mo(CO)_5I]^-$ species with the $[Fe_2S_2(CO)_6]^{2-}$ dianion (see below). (ii) Two new Mo–Fe bonds are formed in the cluster assembly reaction, with that bridged by CO being approximately 0.09 Å shorter than the unbridged one. (iii) The average Mo–S distance of 2.54 Å is 0.1 Å longer than that observed in clusters I and II, which formally contain Mo(II), and approaches the lower end of the range found for the $Mo(CO)_3$-capped hexamers, consistent with formulation of the cluster as containing Mo(0). (iv) As a result of the presence of the metal–metal bonds and bridging carbonyl, the molybdenum is formally eight-coordinate.

This 66e⁻ species is an example of a rare planar mixed-metal cluster and has a structure that contrasts with the previously isolated $Cp'_2Mo_2Fe_2S_2(CO)_8$ (IV) ($Cp' = CH_3C_5H_4$).[39] The latter is a 62e⁻ cluster that, in one isomer, is characterized by two Mo_2Fe units sharing a Mo–Mo edge, with each unit capped by a triply bridging sulfide.[39b] Each molybdenum in III is formally an eight-coordinate Mo(0), whereas each Mo in IV is a nine-coordinate Mo(II).

Formation of Clusters I–III. Clusters I, II-P, and III all contain Mo–Fe–S cores that exhibit unusual coordination geometries. In addition, clusters I and II or II-P appear to have undergone a 2e⁻ oxidation during their formation from $[Fe_2S_2(CO)_6]^{2-}$ and $[Mo(CO)_4I_3]^-$ and $[Mo(CO)_5I]^-$, respectively. Although the formation of an array of complex clusters from two such simple reactions is initially difficult to rationalize, careful consideration of the known chemistry of the $[Fe_2S_2(CO)_6]^{2-}$ dianion[23,24,30] and the Mo–CO–I starting materials results in a plausible description of the chemistry leading to clusters I–III.

Thus, reaction of the $[Fe_2S_2(CO)_6]^{2-}$ ion with $[Mo(CO)_5I]^-$ at low temperature is expected to result in rapid nucleophilic attack

Scheme I

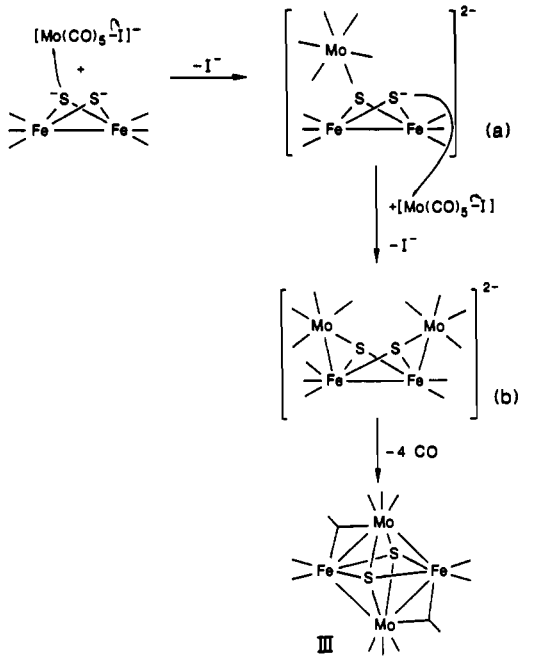

Scheme II

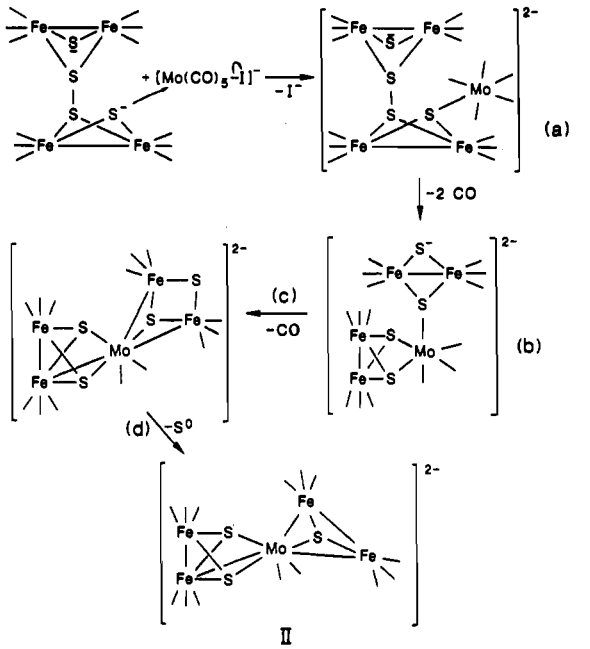

of one of the bridging sulfides of $[Fe_2S_2(CO)_6]^{2-}$ (which are known to be potent nucleophiles) on Mo with loss of I⁻, producing intermediate a in Scheme I. At this point, intramolecular attack of the second sulfide in intermediate a to form a triangular bis(μ_3-sulfido) cluster might be anticipated, but appears to be slow at low temperatures, since CO substitution in such systems is typically a thermally activated dissociative process.[40] Consequently, the intramolecular closure cannot compete with reaction of species a with a second $[Mo(CO)_5I]^-$ to form the tetrametallic intermediate b in Scheme I. Metal–metal bond formation accompanied by loss of CO's and formation of bridging CO's provides a plausible route to cluster III and is analogous to rearrangements previously observed in, e.g., Os–S–CO[41a] cluster chemistry and group VI–S–CO[41b] cluster chemistry.

(39) (a) Braunstein, P.; Jud, J.-M.; Tiripicchio, A.; Tiripicchio-Camellini, M.; Sappa, E. *Angew. Chem., Int. Ed. Engl.* **1982**, *21*, 307. (b) Williams, P. D.; Curtis, M. D.; Duffy, D. N.; Butler, W. M. *Organometallics* **1983**, *2*, 165.

(40) Collman, J. P.; Hegedus, L. S.; Norton, J. R.; Finke, R. G. *Principles and Applications of Organotransition Metal Chemistry*; University Science Books: Mill Valley, CA, 1987; pp 246–253.

(41) (a) Adams, R. D. *Polyhedron* **1985**, *4*, 2003. (b) Darensbourg, D. J.; Zalewski, D. J.; Sanchez, K. M.; Delord, T. *Inorg. Chem.* **1988**, *27*, 821.

Scheme III

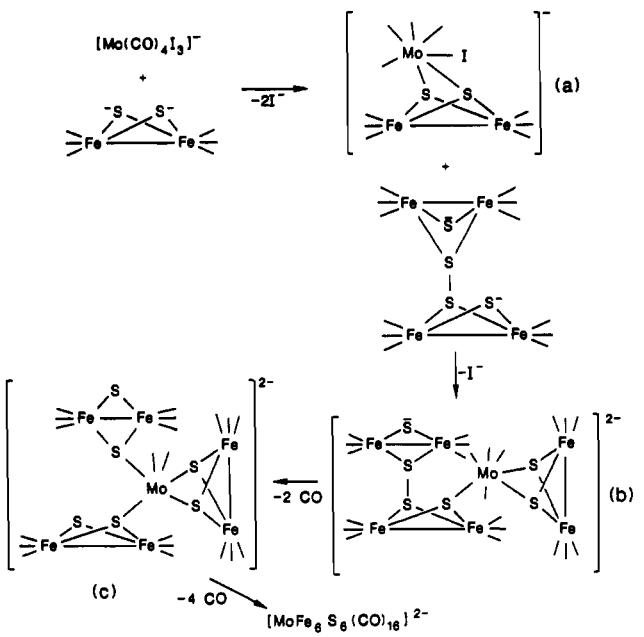

I

The formation of II from $[Mo(CO)_5I]^-$ apparently requires a $2e^-$ oxidation. Although the reaction is carried out in a rigorously anaerobic atmosphere under reducing conditions, our previous work on $[Fe_2S_2(CO)_6]^{2-}$ chemistry suggests a plausible candidate for the oxidant. The $[Fe_4S_4(CO)_{12}]^{2-}$ species (V), consisting of two $Fe_2S_2(CO)_6$ units bridged by an intermolecular disulfide bond (shown schematically at upper left in Scheme II), is known to form upon warming solutions of $[Fe_2S_2(CO)_6]^{2-}$.[30] As a result of the formation of V, a tetrairon species containing 2 oxidizing equiv is formed in situ. Reaction of V with $[Mo(CO)_5I]^-$ should produce an intermediate such as species a in Scheme II, containing a disulfide in close proximity to the Mo(0). Oxidative addition would result in a species such as intermediate b, containing only three sulfides coordinated to Mo. Nucleophilic attack of the remaining sulfide to displace CO is expected to be slow, and metal–metal bond formation and extrusion of elemental sulfur (steps c and d in Scheme II) provide a plausible route to II. Evidence for the chemistry shown in Scheme II is provided by reaction of V (prepared in situ by warming an $[Fe_2S(SH)(CO)_6]^-$ solution to room temperature for several hours,[30] followed by cooling to −78 °C) with $[Mo(CO)_5I]^-$. Monitoring of the FT-IR spectra of the reaction mixture shows that only II is produced under these conditions, with undetectable amounts of III.

Cluster II is also formed from reaction of $[Fe_2S_2(CO)_6]^{2-}$ with the Mo(II) species, $[Mo(CO)_4I_3]^-$, suggesting that intermediate b in Scheme II may also be formed directly from two $[Fe_2S_2(CO)_6]^{2-}$ species and $[Mo(CO)_4I_3]^-$. Alternatively, the fact that clusters II and II-P exhibit quasireversible $2e^-$ oxidation processes at ca. 0 V vs SSCE[42] suggests the possibility that the formation of II from $[Mo(CO)_4I_3]^-$ could proceed analogously to the route shown in Scheme II, producing the $2e^-$-oxidized species $MoFe_4S_3(CO)_{14}$, which is then reduced to II by excess reductant in the reaction mixture.

The formation of cluster I is obviously more complex. A plausible pathway is shown in Scheme III. Attack of $[Fe_2S_2(CO)_6]^{2-}$ on $[Mo(CO)_4I_3]^-$ by displacement of two I^- ions should be facile, resulting in formation of a triangular bis(μ_3-sulfido) cluster intermediate such as species a. Reaction of intermediate a with one sulfide of V, in an analogous fashion to the reaction of V with $[Mo(CO)_5I]^-$, would produce an intermediate (species b) of the appropriate nuclearity containing an appended disulfide. Oxidative addition of the disulfide as in Scheme II would produce a species (intermediate c) containing two "bidentate" and one "monodentate" $Fe_2S_2(CO)_6$ units, which upon Mo–S and Mo–Fe bond formation and loss of CO would produce I. Evidence for the requirement of *both* $[Fe_2S_2(CO)_6]^{2-}$ *and* V for formation of I is provided by experiments such as that discussed above, in which reaction of V with $[Mo(CO)_4I_3]^-$ was shown by FT-IR spectroscopy to produce only II and small amounts of other as yet unidentified clusters, but no I.

Conclusions

(i) Reaction of the $[Fe_2S_2(CO)_6]^{2-}$ dianion with low-valent molybdenum sources results in the formation of a variety of high-nuclearity Mo–Fe–S clusters with unexpectedly complex structures. The complexity of the system is apparently due to competition between reactions involving both the $[Fe_2S_2(CO)_6]^{2-}$ dianion and its $2e^-$-oxidized dimer $[Fe_4S_4(CO)_{12}]^{2-}$ (formed in situ) with the Mo starting material, followed by substantial rearrangements due to formation and/or cleavage of Mo–Fe, Fe–Fe, and Fe–S bonds within the high-nuclearity intermediates.

(ii) The product of one such reaction, the $[MoFe_6S_6(CO)_{16}]^{2-}$ ion (I), is the first synthetic Mo–Fe–S cluster to approximate the core composition and Mo–Fe distance distribution of the FeMo-cofactor of nitrogenase and, as such, constitutes a promising precursor to models for FeMo-co via oxidative decarbonylation reactions. Although the presence of abiological CO ligands in I precludes its consideration as a detailed model for FeMo-co, it is nonetheless the first example of such a low-symmetry synthetic cluster and of a cluster that is completely coordinatively saturated at Mo with no labile ligands. Both of these points may be relevant to the structure of FeMo-co inasmuch as conceptual models proposed to date invariably possess both relatively high symmetry and labile coordination sites at Mo. Evidence for an intrinsically low symmetry structure for FeMo-co has been advanced (but not universally accepted), while a "molybdocentric" view of nitrogenase has long dominated the field, based on initial results suggesting the "unique" requirement of Mo for biological nitrogen fixation.[5] Recent work, however, demonstrating the presence in nature of both a V–Fe nitrogenase[43] (containing an FeV-cofactor cluster[44]) and apparently a nitrogenase containing only Fe,[45] cast doubt on the central role of molybdenum in nitrogen fixation. In fact, the simplest interpretation of the existence of the three nitrogenases may well be that N_2 and other substrates do *not* bind at Mo (or V), but rather at Fe, the only metal site common to all three systems. Clusters such as I demonstrate that it is indeed possible to construct Mo–Fe–S clusters in which the Mo serves as a template around which a particular array of Fe and S atoms may be assembled.

(iii) Synthetic Mo–Fe–S clusters containing Mo in intermediate formal oxidation states (+2 to +4) appear to have a tendency to form new Mo–Fe bonds, resulting in a coordination number of 9 for molybdenum. This is true of all structurally characterized $MoFe_3S_4$ "cubane" complexes,[19a] in which the steric constraints imposed by triply bridging sulfides admittedly make it difficult to assess the extent of Mo–Fe bonding, but is particularly apparent in the structures of I and the "capped-cubane" $MoFe_5S_6(CO)_6(PEt)_3$ cluster[28] recently reported from our laboratory. This apparent tendency to utilize all available Mo valence orbitals occurs only in the absence of strong π-donors (e.g., terminal oxide or sulfide in the $[MoOFe_5S_6(CO)_{16}]^{2-}$[26] and, e.g., $[(RS)_2FeS_2MoS_2]^{2-}$ "linear" clusters)[19a-c,e] or strong π-acids (e.g.,

(42) Eldredge, P. A.; Averill, B. A.; Meyer, T. J. To be submitted for publication.

(43) (a) Bishop, P. E.; Jarlenski, D. M. L.; Hetherington, D. R. *Proc. Natl. Acad. Sci. U.S.A.* **1980**, *77*, 7342; *J. Bacteriol.* **1982**, *150*, 1244. (b) Hales, B. J.; Case, E. E.; Morningstar, J. E.; Dzeda, M. F.; Mauterer, L. A. *Biochemistry* **1986**, *25*, 7251. (c) Eady, R. R.; Robson, R. L.; Richardson, T. H.; Miller, R. W.; Hawkins, M. *Biochem. J.* **1987**, *244*, 197.

(44) (a) Arber, J. M.; Dobson, B. R.; Eady, R. R.; Stevens, P.; Hasnain, S. S.; Garner, C. D.; Smith, B. E. *Nature (London)* **1987**, *325*, 372. (b) Morningstar, J. E.; Hales, B. J. *J. Am. Chem. Soc.* **1987**, *109*, 6854. (c) Morningstar, J. E.; Johnson, M. K.; Case, E. E.; Hales, B. J. *Biochemistry* **1987**, *26*, 1795.

(45) Chisnell, J. R.; Premakumar, R.; Bishop, P. E. *J. Bacteriol.* **1988**, *17*, 27.

compounds II-P and III and the $[Mo(CO)_3Fe_3S_4(SR)_3]^{3-}$ cubane,[22] all of which contain CO ligands to Mo). Since there is no evidence for the presence of either π-acid or terminal oxide or sulfide ligands on Mo in FeMo-co, the above considerations suggest that the Mo site of FeMo-co may well prove to be formally nine-coordinate when its structure is finally determined.

Acknowledgment. We thank Dr. Michal Sabat for assistance with the tables and figures. This research was supported by the National Science Foundation (Grant No. CHE-89-01474) and in part by the U.S. Department of Agriculture SEA/CRGO (Grant No. 86-CRCR-1-2033).

Supplementary Material Available: Tables of positional and thermal parameters and bond lengths and angles for $(Ph_4As)_2(I)$, $(Et_4N)_2(I)$, $(Ph_4As)_2(II\text{-}P)$, and $(Ph_4As)_2(III)$ (38 pages); tables of observed and calculated structure factors for $(Ph_4As)_2(I)$, $(Et_4N)_2(I)$, $(Ph_4As)_2(II\text{-}P)$, and $(Ph_4As)_2(III)$ (102 pages). Ordering information is given on any current masthead page.

Contribution from the Institute for Inorganic Chemistry, University of Witten/Herdecke, Stockumer Strasse 10, 5810 Witten, Federal Republic of Germany

Kinetics and Mechanism of the Sulfite-Induced Autoxidation of Cobalt(II) in Aqueous Azide Medium

Nina Coichev[1] and Rudi van Eldik*

Received November 27, 1990

The autoxidation of Co(II) in azide medium is accelerated by sulfur(IV) oxides at a concentration level of 10^{-5} M. The formation of Co(III) was followed spectrophotometrically under the following conditions: [Co(II)] = 5×10^{-4} M; initial [Co(III)] = (0–3.6) $\times 10^{-5}$ M; [total S(IV)] = (1–4) $\times 10^{-5}$ M; $4 < pH < 6$; [total N_3^-] = 0.1–0.5 M; temperature = 25 °C; ionic strength = 1.0 M. The autoxidation reaction exhibits typical autocatalytic behavior in which the induction period depends on the Co(III) concentration. A detailed kinetic study of both the autoxidation step and the reduction of Co(III) by sulfur(IV) oxides demonstrates that the same rate-determining step is operative in both cases. This step involves the reduction of Co(III) by sulfur(IV) oxide to produce the SO_3^- radical, which reacts with dissolved oxygen to produce SO_5^- and rapidly oxidizes Co(II) in at least two consecutive steps. The observed rate constant depends on the pH and azide concentration, since these control the speciation of the sulfur(IV) oxides and cobalt(II/III) azide complexes. The proposed mechanism is discussed in reference to available literature information.

Introduction

We are in general interested in the metal-catalyzed autoxidation mechanism of sulfur(IV) oxides and its role in atmospheric oxidation processes, i.e. the formation of acid rain. We have in the past undertaken a detailed study of the Fe(III)-catalyzed autoxidation reactions[2-4] and are presently investigating the catalytic role of some model Fe(III) complexes.[5] A crucial step in the overall oxidation mechanism[4] concerns the oxidation of Fe(II) that is produced during the oxidation of sulfur(IV) oxides by Fe(III). Such oxidation reactions are usually slow, but it has been suggested[6] and recently found in our laboratories[7] that the autoxidation of Fe(II) is catalyzed by sulfur(IV) oxides. In this respect it should be noted that evidence for the formation of a strong oxidant (most likely SO_5^{2-} and HSO_5^-) in the reaction of SO_3^{2-} with O_2 has been reported.[8] This oxidant plays an important role in mineral extraction processes.

In the present study we have investigated the kinetics and mechanism of the sulfite-catalyzed autoxidation of Co(II) in the presence of azide. It is generally known that cobalt(II) azide complexes are oxidized slowly by dissolved oxygen to the corresponding Co(III) complexes. However, this reaction is markedly accelerated by sulfur(IV) oxides (SO_2, HSO_3^-, SO_3^{2-}), such that it can be employed as a spot test for sulfite[9,10] and as a quantitative analytical method.[11] Preliminary measurements demonstrated that the S(IV)-catalyzed autoxidation reaction exhibits typical autocatalytic behavior that depends on the presence of Co(III) species.[11,12] It was therefore the major objective of this study to resolve the underlying reaction mechanism and so contribute toward the understanding of the catalyzed autoxidation process. At the same time we are convinced that similar reactions occur in the sulfite-catalyzed autoxidation of Fe(II) mentioned above.[7]

Experimental Section

All reagents were of analytical reagent grade (Merck), and deionized water was used to prepare all solutions. N_2 was used to deaerate solutions where required. Stock solutions of sulfite were prepared by dissolving $Na_2S_2O_5$ in deaerated water and kept in a refrigerator at 5 °C ($S_2O_5^{2-}$ dissociates in water to HSO_3^-; see ref 2). Other stock solutions were prepared by using NaN_3, $HClO_4$ (to adjust the pH), $NaClO_4$ (to adjust the ionic strength to 1.0 M), and $Co(ClO_4)_2$. $Na_3[Co(CO_3)_3]\cdot 3H_2O$ was prepared as described in the literature[13] and used as source of Co(III). When this complex is dissolved in acidic azide buffer medium under the selected experimental conditions, it rapidly aquates via decarboxylation to produce the cobalt(III) azide complex.

UV–vis spectra were recorded on a Shimadzu UV 250 spectrophotometer, which was also used for kinetic measurements in its thermo-

(1) On leave from the Instituto de Quimica, Universidade de Sao Paulo, Sao Paulo, Brazil.
(2) Kraft, J.; van Eldik, R. *Inorg. Chem.* **1989**, *28*, 2297.
(3) Kraft, J.; van Eldik, R. *Inorg. Chem.* **1989**, *28*, 2306.
(4) Kraft, J.; van Eldik, R. *Atmos. Environ.* **1989**, *23*, 2709.
(5) Dellert-Ritter, M.; van Eldik, R. Submitted for publication.
(6) Sato, T.; Goto, T.; Okabe, T.; Lawson, F. *Bull. Chem. Soc. Jpn.* **1984**, *57*, 2082.
(7) Bal Reddy, K.; Coichev, N.; van Eldik, R. *J. Chem. Soc., Chem. Commun.*, in press.
(8) Devuyst, E. A. P.; Ettel, V. A.; Mosolu, M. A. CHEMTECH **1979**, 426.
(9) Senise, P. *Mikrochim. Acta* **1957**, *5*, 640.
(10) Feigl, F.; Anger, V. *Spot Tests in Inorganic Analysis*, 6th ed.; Elsevier: Amsterdam, 1972; p 447.
(11) Neves, E. A.; Gebert, J.; Klockow, D. *Fresenius' Z. Anal. Chem.* **1988**, *331*, 260.
(12) Neves, E. A.; Coichev, N.; Gebert, J.; Klockow, D. *Fresenius' Z. Anal. Chem.* **1989**, *335*, 386.
(13) Bauer, H. F.; Drinkard, W. C. *Inorganic Syntheses*; McGraw Hill Book Co.: New York, 1966; Vol. 8, pp 202–204.

0020-1669/91/1330-2375$02.50/0